

# Field Theory of Critical Behaviour in Driven Diffusive Systems with Quenched Disorder

V. Becker and H.K. Janssen  
 Institut für Theoretische Physik III  
 Heinrich-Heine-Universität Düsseldorf  
 D-40225 Düsseldorf, Germany

March 22, 1998

We present a field theoretic renormalization group study for the critical behaviour of a uniformly driven diffusive system with quenched disorder, which is modelled by different kinds of potential barriers between sites. Due to their symmetry properties, these different realizations of the random potential barriers lead to three different models for the phase transition to transverse order and to one model for the phase transition to longitudinal order all belonging to distinct universality classes. In these four models that have different upper critical dimensions  $d_c$  we find the critical scaling behaviour of the vertex functions in spatial dimensions  $d < d_c$ . Its deviation from purely diffusive behaviour is characterized by the anomaly-exponent  $\eta$  that we calculate at first and second order, respectively in  $\epsilon = d_c - d$ . In each model  $\eta$  turns out to be positive which means superdiffusive spread of density fluctuations in the driving force direction.

# 1 Introduction

For more than a decade the long-time and critical behaviour of diffusive systems subjected to a driving force has attracted considerable interest. This is mainly caused by the richness of their highly nontrivial features which generically result from the fact that, due to the driving force, in general even the steady states of these systems are far from thermal equilibrium, especially in the case of very strong driving forces. Further, driven diffusive systems might be suitable models for fast ionic conductors which was first suggested by Katz, Lebowitz, and Spohn [1,2]. A review of the different investigations on driven diffusive systems and their relations to other non-equilibrium systems is given by Schmittmann and Zia [3].

We are interested in the diffusive motion of uniformly driven particles with short range attractive interactions and hardcore repulsion. With such an interaction driven diffusive systems show two kinds of phase transitions. At the transverse (with respect to the driving force  $\mathbf{E}$ ) phase transition the system changes from a disordered state to an ordered one where the system is ordered in the transverse direction and remains disordered in the longitudinal (parallel to the driving force) direction. The typical configurations are strips of high- and low-density phase, arranged parallel to the driving force  $\mathbf{E}$  (Fig. 1(a)). At the longitudinal phase transition the systems changes from a disordered state to a state where the system is ordered in the longitudinal direction and remains disordered in the transverse directions. Here the typical configurations are domains ("pancakes") of different phase with interfaces perpendicular to the driving force (Fig. 1(b)). In preceding papers the long-time and critical behaviour of driven diffusion in an ordered medium [4–6] and the long-time behaviour of driven diffusion in a medium with quenched disorder [7] have been investigated by renormalized field theory. In the present paper we study the effect of quenched disorder on the two kinds of phase transitions in driven diffusive systems. Quenched disorder is important in real systems, as it models impurities and defects. We stress that this work completes the investigations of a whole model class that is graphically shown in the summary (Fig. 3). Note that the effects of quenched disorder in randomly driven diffusive systems were recently analyzed [8,9]. There the driving force is itself a locally random variable with respect to its amplitude and sign, whereas here the driving force is uniform.

The paper is organized as follows: In Section II we set up a Langevin description of our system, directly on a mesoscopic length scale using conservation

laws and symmetry arguments. The quenched disorder is modelled by random potential barriers between sites, and the symmetry properties of the random potential play a crucial role. Different realizations of the random potential are possible and are argued to lead to different kinds of noise. In Section III we study the transverse phase transition in the convenient formalism of the dynamic functional. In Section IV the longitudinal phase transition is analyzed. Section V contains the main results and a graphical overview of the entire model class.

## 2 Model Building

The configurations of a driven diffusive system with homogenous driving force are fully characterized by a single conserved scalar field, i.e., the local particle density  $n(\mathbf{r}, t)$ . As the particle number is conserved the order parameter for both phase transitions is the deviation of the actual density  $n(\mathbf{r}, t)$  from its uniform average  $n_0$ :

$$s(\mathbf{r}, t) = n(\mathbf{r}, t) - n_0 . \quad (1)$$

This fluctuating variable satisfies a continuity equation

$$\dot{s} + \nabla \cdot \mathbf{j} = 0 \quad (2)$$

where the current density  $\mathbf{j}$  consists of a deterministic and a random part. The resulting stochastic differential equation is a Langevin equation. First we model the deterministic part. Due to the anisotropy of the system caused by the driving force,  $\mathbf{j}$  shows different symmetries longitudinal and transverse to its direction. Henceforth the indices  $\parallel$  and  $\perp$  denote the spatial direction longitudinal to the driving force and the  $(d - 1)$ -dimensional subspace transverse to it, respectively. The transverse current is according to

$$\mathbf{j}_\perp = -\lambda \nabla_\perp \mu_\perp \quad (3)$$

caused by a chemical potential  $\mu_\perp$  with  $\lambda$  being a kinetic coefficient. As no direction is selected in the  $(d - 1)$ -dimensional subspace the transverse current  $\mathbf{j}_\perp$  is isotropic and therefore a vector of the form

$$\mathbf{j}_\perp = \nabla_\perp f(s, \Delta_\perp, \nabla_\parallel) \quad (4)$$

where the Laplacean  $\Delta_\perp$  as argument denotes an even number of  $\nabla_\perp$ -operators in every term of  $f$ . An expansion of  $f$  with respect to  $s$  and gradient-operators yields, up to higher order terms

$$\mathbf{j}_\perp = \nabla_\perp (s + s^2 + \Delta_\perp s + \nabla_\parallel s + \Delta_\parallel s) , \quad (5)$$

where here and in the following equations coefficients are suppressed for the sake of simplicity.

The longitudinal current, however, possesses no symmetry, due to the driving force. As a scalar it can be written as

$$j_\parallel = g(s, \nabla_\parallel, \Delta_\perp) \quad (6)$$

where the isotropy of the transverse subspace is again taken into account by the even number of  $\nabla_{\perp}$ -operators. Its expansion up to higher order terms reads

$$j_{\parallel} = c + s + s^2 + \nabla_{\parallel}s + \nabla_{\parallel}^2s + \nabla_{\parallel}^3s + \nabla_{\parallel}s^2 + \Delta_{\perp}s + \nabla_{\parallel}\Delta_{\perp}s. \quad (7)$$

While some terms in this equation originate in a chemical potential  $\mu_{\parallel}$ , according to

$$j_{\parallel} = -\lambda \nabla_{\parallel} \mu_{\parallel}, \quad (8)$$

others are due to the driving force  $\mathbf{E}$ , which at least produces the terms proportional to  $c$ ,  $s$ ,  $s^2$ , and  $\Delta_{\perp}s$  and which, in principle, also contributes to all terms of the longitudinal current in (7). Here, the constant  $c$  is the homogenous part of the current, and  $s^2$  is the first nonlinear term of the longitudinal current and so the leading nonlinearity of the problem.

Note that a repeated coarse graining of a microscopic model typically generates anisotropic transport coefficients. Building here a model directly on a mesoscopic length scale we must take that into consideration. Thus, although containing the same terms,  $\mu_{\parallel}$  and  $\mu_{\perp}$  in general have different coefficients, due to the anisotropy. From a technical point of view anisotropic transport coefficients are required to make the model renormalizable.

Following microscopic models and simulations [1, 2, 10–12] we restrict ourselves to such models which additionally hold a CP (charge and parity)-symmetry, i.e. in which the Langevin equation is invariant under the transformation

$$s(r_{\parallel}, \mathbf{r}_{\perp}, t) \rightarrow -s(-r_{\parallel}, \mathbf{r}_{\perp}, t). \quad (9)$$

In microscopic lattice models which also form the basis for Monte Carlo simulations of driven diffusive systems the PC-symmetry corresponds to the particle-hole symmetry in the half-filled system.

In models with PC-symmetry all terms from (5) and (7) vanish whose sum of  $s$ - and  $\nabla_{\parallel}$ -factors in the Langevin equation is even.

The stochastic part of the Langevin equation  $\zeta = -\nabla \cdot \mathbf{j}_L$  reflects a random current  $\mathbf{j}_L$  that summarizes the fast microscopic degrees of freedom (local in time in our Markovian continuum description) and the effects of the quenched disorder of the medium. After writing down the general form of the Langevin equation we show how to model the various possibilities of quenched disorder and which parts of the noise are relevant in the renormalization group sense. Note that the noise considered here is conserving, i.e., it satisfies the continuity equation. We mention that we have also analyzed driven diffusive systems

with nonconserving noise that is caused by random particle sources [13, 14]. Taking anisotropic transport coefficients into account we obtain the Langevin equation

$$\dot{s} = \lambda[\Delta_{\perp}(\tau_{\perp} - \kappa_{\perp}\Delta_{\perp}) + \rho\Delta_{\parallel}(\tau_{\parallel} - \kappa_{\parallel}\Delta_{\parallel}) - \kappa\Delta_{\perp}\Delta_{\parallel}]s + \frac{1}{2}\lambda g\nabla_{\parallel}s^2 - \nabla \cdot \mathbf{j}_L. \quad (10)$$

This constitutes the fundamental equation for driven diffusive systems with homogenous driving force, attractive interactions, CP-symmetry and conserving noise. It contains all terms which are relevant in the renormalization group sense for the two phase transitions and the noncritical disordered phase, but in each case it still contains irrelevant terms which must be eliminated by a dimensional analysis.

We proceed by investigating the influence of the quenched disorder in detail. In a microscopic driven lattice gas model the quenched disorder is modelled by random potential barriers between the sites. There are three possible realizations of their randomness which is depicted for one dimensional systems in Fig. 2.

- I The particles are in randomly deep potential valleys that are separated by randomly high potential mountains (Fig. 2 (a)).
- II The potential valleys are randomly deep, the potential mountains are equally high (Fig. 2 (b)).
- III The potential mountains are randomly high, but the potential valleys are equally deep (Fig. 2 (c)).

The homogeneous driving force tilts this landscape in the longitudinal direction by an angle that depends on its strength. Thus in this direction the symmetry of the random potential in the realizations II and III is broken, whereas the symmetries in the transverse subspace are not affected. Hence in the driving force direction the random potential is unsymmetric in all realizations.

In the microscopic lattice gas model particles can only jump to neighbouring unoccupied sites with jump rates that depend on the external driving force, on the energetic situation of the particles due to their attractive interaction, and on the locally random height of the potential barriers between the sites. Performing a continuum limit of the microscopic model one can show that, first, the main effect of the quenched disorder results in a time-independent

random current with zero mean and Gaussian fluctuations and that, second, the three different realizations of the random potential produce three different types of such a random current  $\zeta_d(\mathbf{r})$ .

In the unsymmetric case (realization I) the correlations of the random current are given by

$$\begin{aligned} \langle \zeta_d(\mathbf{r}) \rangle &= 0 \\ \langle \zeta_d(\mathbf{r}) \otimes \zeta_d(\mathbf{r}') \rangle &= 2\lambda^2 \delta(\mathbf{r} - \mathbf{r}') [\sigma \mathbf{e}_{\parallel} \otimes \mathbf{e}_{\parallel} + \gamma (\mathbf{1} - \mathbf{e}_{\parallel} \otimes \mathbf{e}_{\parallel})] . \end{aligned} \quad (11)$$

Thus the correlations of the noise force  $\nabla \cdot \zeta_d$  read

$$\begin{aligned} \langle \nabla \cdot \zeta_d(\mathbf{r}) \rangle &= 0 \\ \langle \nabla \cdot \zeta_d(\mathbf{r}) \nabla \cdot \zeta(\mathbf{r}') \rangle &= -2\lambda^2 (\gamma \Delta_{\perp} + \sigma \Delta_{\parallel}) \delta(\mathbf{r} - \mathbf{r}') . \end{aligned} \quad (12)$$

By a suitable scale change of  $s$  the kinetic coefficient  $\lambda$  in equation(12) is the same as in equation(10). The anisotropy of the system due to the driving force is taken into account here by the transport coefficients  $\gamma$  and  $\sigma$ .

In realization II a particle at a given site sees equally high potential barriers in all transverse directions. As a consequence of this symmetry the random current in the transverse subspace vanishes in the lowest order and starts with a local gradient. The correlations of the random current are here given by

$$\langle \nabla \cdot \zeta(\mathbf{r}) \nabla \cdot \zeta(\mathbf{r}') \rangle = -2\lambda^2 (-\alpha \Delta_{\perp}^2 + \sigma \Delta_{\parallel}) \delta(\mathbf{r} - \mathbf{r}') . \quad (13)$$

As the symmetry of the random potential is broken by the driving force in the longitudinal direction the longitudinal random current behaves as in the unsymmetric case.

In realization III a potential barrier looks the same from both sides in the transverse subspace. This is why the transverse random current vanishes totally. Being only longitudinal the random current has the correlations

$$\langle \nabla \cdot \zeta(\mathbf{r}) \nabla \cdot \zeta(\mathbf{r}') \rangle = -2\lambda^2 \sigma \Delta_{\parallel} \delta(\mathbf{r} - \mathbf{r}') . \quad (14)$$

Since the continuum limit of the microscopic model is not rigorous, it might be possible that even in the symmetric realizations II and III transverse noise terms with  $\alpha \neq 0$  and  $\gamma \neq 0$ , respectively, are generated by the coarse graining procedure. This is due to the fact that the symmetry of the random potential is microscopic and concerns only a single site or bond. As we will see later each type of noise nevertheless leads to different critical behaviour

governed by different stable fixed points with finite regions of attraction. We defer the discussion of the possible additional transverse noise terms until the end of the Sections 3.2 and 3.3, respectively.

By dimensional considerations (power counting) one can prove that each of the equations (12) – (14) contains all relevant noise terms in the renormalization group sense for the respective type of the random potential. Also deviations from the local Gaussian nature of the random current  $\zeta$  are irrelevant for the critical and long-time properties. Even the microscopic part  $\zeta_m$  of the random current summarizing the fast microscopic degrees of freedom is irrelevant if  $\zeta_d \neq 0$ . It should be remarked that  $\zeta_m$  plays the role of a dangerous irrelevant field for the calculation of correlation functions with frequencies  $\omega \neq 0$ . Without  $\zeta_m$  correlation functions show only a "central peak" at  $\omega = 0$ .



### 3 Transverse Phase Transition

In the following all models are analyzed with the help of renormalized field theory. This method has successfully been applied to all driven diffusive models investigated so far.

The three different realizations of the random potential described in the last section actually lead to three different models for the transverse phase transition and have to be treated separately.

#### 3.1 Unsymmetric Random Potential

The model for a driven diffusive system with frozen random unsymmetric potential is based on the equations (10) and (12).

To set up a renormalized field theory, it is convenient to recast the model in terms of a dynamic functional [15–20]

$$\mathcal{J}[s, \tilde{s}] = \int d^d r \left\{ \int dt [\tilde{s} (\dot{s} + \lambda(\Delta_\perp(\kappa_\perp \Delta_\perp - \tau_\perp) + \rho \Delta_\parallel(\kappa_\parallel \Delta_\parallel - \tau_\parallel) + \kappa \Delta_\perp \Delta_\parallel) s) + \frac{1}{2} \lambda g (\nabla_\parallel \tilde{s}) s^2] - \gamma \left[ \lambda \int dt \nabla_\perp \tilde{s} \right]^2 - \sigma \left[ \lambda \int dt \nabla_\parallel \tilde{s} \right]^2 \right\}, \quad (15)$$

where  $\tilde{s}(\mathbf{r}, t)$  is a Martin–Siggia–Rose [21] response field. Correlation and response functions can now be expressed as functional averages with weight  $\exp(-\mathcal{J})$ .

But for the description of the transverse phase transition this dynamic functional still contains irrelevant terms in the renormalization group sense. Now these terms are determined by a dimensional analysis.

The transverse phase transition is characterized by finite  $\tau_\parallel$  and  $\tau_\perp \rightarrow 0$ . We introduce a scale  $\mu^2$  for small  $\tau_\perp$ . Then  $\mu^{-1}$  is a convenient length scale. Since  $\tau_\perp$  tends to 0 at the transverse phase transition, the leading term in the transverse direction is proportional to  $\tilde{s} \lambda \Delta_\perp \kappa_\perp \Delta_\perp s$ , whereas in the longitudinal direction the leading gradient term is proportional to  $\tilde{s} \lambda \rho \Delta_\parallel \tau_\parallel s$ . The comparison of the leading gradient terms demonstrates that  $\Delta_\parallel$  scales as  $\Delta_\perp^2$ . For longitudinal and transverse length scales, this implies

$$r_\perp \sim \mu^{-1} \quad r_\parallel \sim \mu^{-2}. \quad (16)$$

Since the dynamic functional is dimensionless the dimensions of fields and coupling constants are

$$\lambda t \sim \mu^{-4} \quad s \sim \mu^{\frac{d-5}{2}} \quad \tilde{s} \sim \mu^{\frac{d+7}{2}}$$

$$\begin{aligned}
\kappa_{\parallel} &\sim \mu^{-4} & \kappa &\sim \mu^{-2} & \sigma &\sim \mu^{-2} \\
\gamma &\sim \mu^0 & g &\sim \mu^{\frac{9-d}{2}}, & & 
\end{aligned} \tag{17}$$

i.e. the coupling constants  $\kappa_{\parallel}$ ,  $\kappa$ , and  $\sigma$  are irrelevant in the renormalization group sense. The irrelevancy of  $\sigma$  indicates that for the transverse phase transition in a unsymmetric random potential the noise in the driving force direction is irrelevant. From the dimension of the nonlinear coupling constant  $g$  we recognize

$$d_c = 9 \tag{18}$$

as upper critical dimension of this model, above which  $g$  is irrelevant and below which  $g$  is relevant. The finite  $\tau_{\parallel}$  and the transverse coupling constants are absorbed into lengths and fields by a suitable scale change. Thus, the appropriate dynamic functional to describe the transverse phase transition in a driven diffusive system with an unsymmetric random potential is given by

$$\begin{aligned}
\mathcal{J}[s, \tilde{s}] = & \int d^d r \left\{ \int dt \left[ \tilde{s} \dot{s} + \lambda \tilde{s} (\Delta_{\perp} (\Delta_{\perp} - \tau_{\perp}) - \rho \Delta_{\parallel}) s + \frac{1}{2} \lambda g (\nabla_{\parallel} \tilde{s}) s^2 \right] \right. \\
& \left. - \left[ \lambda \int dt \nabla_{\perp} \tilde{s} \right]^2 \right\}. \tag{19}
\end{aligned}$$

The dynamic functional has the following symmetries. The isotropy in the transverse subspace and the CP-symmetry that reads here

$$r_{\parallel} \rightarrow -r_{\parallel} \quad s \rightarrow -s \quad \tilde{s} \rightarrow -\tilde{s} \tag{20}$$

were directly integrated in the model building. After averaging over the quenched disorder,  $\mathcal{J}$  exhibits translational symmetry in space and time. The invariance of  $\mathcal{J}$  under the longitudinal scale transformation

$$\begin{aligned}
r_{\parallel} &\rightarrow \beta r_{\parallel} & r_{\perp} &\rightarrow r_{\perp} \\
\tilde{s} &\rightarrow \beta^{-\frac{1}{2}} \tilde{s} & s &\rightarrow \beta^{-\frac{1}{2}} s \\
\rho &\rightarrow \beta^2 \rho & g &\rightarrow \beta^{\frac{3}{2}} g
\end{aligned} \tag{21}$$

is of great importance, because the parameter combination  $g^2 \rho^{-\frac{3}{2}}$  is found as appropriate variable of the model being invariant under this transformation. In contrast to the corresponding model without quenched disorder [5] the dynamic functional is here not invariant under a Galilei transformation.

To study the critical properties of the transverse phase transition we apply standard renormalization group methods [19, 20, 22]. We use dimensional regularization in  $d = 9 - \epsilon$  followed by minimal subtraction. The one-line-irreducible vertex functions with  $\tilde{n}$   $\tilde{s}$ -legs and  $n$   $s$ -legs at wavevectors  $\{\mathbf{q}\}$  and frequencies  $\{\omega\}$  will be denoted by  $\Gamma_{\tilde{n},n}(\{\mathbf{q}\}, \{\omega\})$ . Taking into consideration the causality properties of the theory we only find  $\Gamma_{1,1}$  and  $\Gamma_{1,2}$  primitively divergent. The nontrivial diagrams contributing to  $\Gamma_{\tilde{n},n}(\{\mathbf{q}\}, \{\omega\})$  carry at least a factor  $q_{\parallel}^{\tilde{n}}$ , because the interaction vertex is conserving. The primitive divergences are multiplicatively absorbed in a redefinition of the parameters

$$\rho \rightarrow \dot{\rho} = Z_{\rho}\rho, \quad g \rightarrow \dot{g} = \mu^{\frac{\epsilon}{2}} Z_u u. \quad (22)$$

Here, in contrast to the ordered problem [5], the coupling constant  $g$  has to be renormalized, due to the loss of Galilean invariance in the disordered problem.

The elements of our perturbation expansion are the Gaussian propagator

$$G_{\mathbf{q},\omega} := \langle \tilde{s}_{\mathbf{q},\omega} s_{-\mathbf{r},-\omega} \rangle_0 = \frac{1}{i\omega + \lambda[\mathbf{q}_{\perp}^2(\mathbf{q}_{\perp}^2 + \tau_{\perp}) + \rho q_{\parallel}^2]}, \quad (23)$$

the Gaussian correlator

$$C_{\mathbf{q},\omega} := \langle s_{\mathbf{q},\omega} s_{-\mathbf{q},-\omega} \rangle_0 = \frac{2\lambda^2 \mathbf{q}_{\perp}^2 \delta(\omega)}{\omega^2 + \lambda^2[\mathbf{q}_{\perp}^2(\mathbf{q}_{\perp}^2 + \tau_{\perp}) + \rho q_{\parallel}^2]^2}, \quad (24)$$

and the conserving vertex  $v(\mathbf{q}) = -i\lambda g q_{\parallel}$ . Their graphical representation is shown in the Appendix in fig.(4).

As the correlator of the theory  $C_{\mathbf{q},\omega}$  is proportional to  $\delta(\omega)$  (i.e.  $C_{\mathbf{q}}(t)$  is independent of time) and any loop of a diagram contains at least one correlator because of the structure of the vertex with two  $s$ -legs and one  $\tilde{s}$ -leg and because of causality the integration over internal frequencies cannot generate any divergences. Thus the divergent parts of the vertex functions are only in the  $(\omega = 0)$ -parts. To facilitate their calculation it is convenient to split the order parameter

$$s(\mathbf{r}, t) = \varphi(\mathbf{r}) + s'(\mathbf{r}, t) \quad (25)$$

into a time independent  $\varphi(\mathbf{r})$  and a time dependent  $s'(\mathbf{r}, t)$  that contains no  $(\omega = 0)$ -parts. Since the noise is independent of time  $s'(\mathbf{r}, t)$  relaxes deterministically. In the limit of long times we obtain

$$s(\mathbf{r}, t \rightarrow \infty) = \varphi(\mathbf{r}). \quad (26)$$

Together with

$$\tilde{\varphi}(\mathbf{r}) = \lambda \int dt \tilde{s}(\mathbf{r}, t) \quad (27)$$

the dynamic functional  $\mathcal{J}$  reduces to a quasi-static (frozen) Hamiltonian

$$\mathcal{H}[\varphi, \tilde{\varphi}] = \int d^d r \left\{ \tilde{\varphi}(\Delta_\perp(\Delta_\perp - \tau_\perp) - \rho\Delta_\parallel)\varphi + \frac{1}{2}g(\nabla_\parallel\tilde{\varphi})\varphi^2 + \tilde{\varphi}\Delta_\perp\tilde{\varphi} \right\} . \quad (28)$$

The frozen Hamiltonian generates all the zero-frequency parts of the vertex functions if causality is included in the graphical rules of perturbation theory. In the quasi-static model the Gaussian propagator and correlator are only dependent on wavevectors and read

$$\begin{aligned} G_{\mathbf{q}} &= \frac{1}{\mathbf{q}_\perp^2(\mathbf{q}_\perp^2 + \tau_\perp) + \rho q_\parallel^2} \\ C_{\mathbf{q}} &= \frac{2\mathbf{q}_\perp^2}{[\mathbf{q}_\perp^2(\mathbf{q}_\perp^2 + \tau_\perp) + \rho q_\parallel^2]^2} . \end{aligned} \quad (29)$$

In the quasi-static model we calculate the primitively divergent vertex functions in two-loop order. While the one-loop calculation is easy to perform analytically, technical difficulties have to be overcome for the two-loop diagrams with mixed  $\mathbf{q}^4$ -propagators and -correlators. These two-loop diagrams have here been solved by a new technique where a special inverse Mellin transformation is used to factorize the denominators of some propagators and correlators, respectively. Thus, the  $\epsilon^2$ -poles and the simple  $\epsilon$ -poles can be extracted. Their coefficients are then given by parameter integrations over paths in the complex plane. Whereas the coefficients of the  $\epsilon^2$ -poles can be analytically calculated, those of the simple  $\epsilon$ -poles have to be computed numerically. The details of the two-loop calculation are shown in the Appendix.

In a two-loop calculation using dimensional regularization we obtain the vertex functions in an expansion in  $\epsilon = d_c - d$  and  $\mathbf{q}$

$$\begin{aligned} \mathring{\Gamma}_{1,1}(\mathbf{q}) &= \mathbf{q}_\perp^2(\mathbf{q}_\perp^2 + \tau_\perp) + \rho q_\parallel^2 + \frac{2}{3} \frac{A_\epsilon}{\epsilon} \frac{\mathring{g}^2}{\rho^{\frac{1}{2}}} q_\parallel^2 \tau_\perp^{-\frac{\epsilon}{2}} - \frac{2}{9} \frac{A_\epsilon^2}{\epsilon^2} \frac{\mathring{g}^4}{\rho^2} q_\parallel^2 \tau_\perp^{-\epsilon} (1 - 0.2158\epsilon) \\ \mathring{\Gamma}_{1,2}(\mathbf{q}) &= i \mathring{g} q_\parallel - i \frac{1}{6} \frac{A_\epsilon}{\epsilon} \frac{\mathring{g}^3}{\rho^{\frac{3}{2}}} q_\parallel \tau_\perp^{-\frac{\epsilon}{2}} + \frac{1}{8} i \frac{A_\epsilon^2}{\epsilon^2} \frac{\mathring{g}^5}{\rho^3} q_\parallel \tau_\perp^{-\epsilon} (1 - 0.2154\epsilon) , \end{aligned} \quad (30)$$

where bare unrenormalized parameters are indicated by a superscript “ $\circ$ ” above the symbol.  $A_\epsilon = \frac{1}{(2\pi)^d} \mathcal{O}_{d-1} \Gamma(1 + \frac{\epsilon}{2}) \Gamma(\frac{5-\epsilon}{2}) \Gamma(\frac{1}{2})$  is a suitably chosen

constant with  $\mathcal{O}_{d-1}$  being the surface of the  $(d-1)$ -dimensional unit sphere and  $\Gamma(z)$  denoting Euler's  $\Gamma$ -function. The  $Z$ -factors defined in equation(22) are in minimal subtraction

$$\begin{aligned} Z_\rho &= 1 - \frac{2}{3\epsilon} A_\epsilon \frac{u^2}{\rho^{\frac{3}{2}}} - \frac{2}{9\epsilon^2} A_\epsilon^2 \frac{u^4}{\rho^3} (1 + 0.2158\epsilon) + \mathcal{O}(u^6) \\ Z_u &= 1 + \frac{1}{6\epsilon} A_\epsilon \frac{u^2}{\rho^{\frac{3}{2}}} + \frac{1}{8\epsilon^2} A_\epsilon^2 \frac{u^4}{\rho^3} (1 + 0.2154\epsilon) + \mathcal{O}(u^6) . \end{aligned} \quad (31)$$

We recognize that the perturbation expansion is organized in powers of the dimensionless renormalized parameter combination  $v := A_\epsilon u^2 \rho^{-\frac{3}{2}}$  that was already found as invariant variable under the longitudinal scale transformation (equation(21)).

With the renormalizations at hand we are in a position to determine the critical behaviour of the vertex functions. We use the fact that the unrenormalized theory is independent of the momentum scale  $\mu$ . This leads to the renormalization group equation

$$\left[ \beta_v \frac{\partial}{\partial v} + \rho \zeta \frac{\partial}{\partial \rho} + \mu \frac{\partial}{\partial \mu} \right] \Gamma_{\tilde{n},n}(\{q_\parallel, \mathbf{q}_\perp\}, \tau_\perp, v, \rho, \mu) = 0 . \quad (32)$$

The Wilson parameter functions, being only dependent on  $v$ , are given by

$$\begin{aligned} \beta_v &:= \left. \mu \frac{\partial v}{\partial \mu} \right|_o = -v \left( \epsilon - \frac{4}{3}v - 0.252v^2 + \mathcal{O}(v^3) \right) \\ \zeta &:= \left. \mu \frac{\partial \ln \rho}{\partial \mu} \right|_o = -\frac{2}{3}v - 0.0959v^2 + \mathcal{O}(v^3) , \end{aligned} \quad (33)$$

where the derivatives are calculated at fixed bare parameters. As a linear partial differential equation the renormalization group equation is solvable by the method of characteristics with the result

$$\Gamma_{\tilde{n},n}(\{q_\parallel, \mathbf{q}_\perp\}, \tau_\perp, v, \rho, \mu) = \Gamma_{\tilde{n},n}(\{q_\parallel, \mathbf{q}_\perp\}, \tau_\perp, \bar{v}(l), \bar{\rho}(l), \bar{\mu}(l)) . \quad (34)$$

The trajectories  $\bar{v}(l)$ ,  $\bar{\rho}(l)$ , and  $\bar{\mu}(l)$  are solutions of the flow equations

$$l \frac{d}{dl} \bar{v}(l) = \beta_v(\bar{v}(l)) \quad l \frac{d}{dl} \ln \bar{\rho}(l) = \zeta(\bar{v}(l)) \quad l \frac{d}{dl} \bar{\mu}(l) = \bar{\mu}(l) \quad (35)$$

with the flow parameter  $l$  and the initial conditions

$$\bar{v}(l=1) = v \quad \bar{\rho}(l=1) = \rho \quad \bar{\mu}(l=1) = \mu . \quad (36)$$

The third flow equation obviously has the solution  $\bar{\mu}(l) = \mu l$ .

With the help of characteristics the critical asymptotic region of small  $\tau_\perp$  and  $q$  can be mapped onto uncritical regions. In the scaling limit  $l \ll 1$  corresponding to

$$\left| \frac{q_\parallel}{\mu^2} \right| \ll 1 \quad \left| \frac{\mathbf{q}_\perp}{\mu} \right| \ll 1 \quad \left| \frac{\tau_\perp}{\mu^2} \right| \ll 1 \quad (37)$$

the flow of  $\bar{v}(l)$  is controlled by stable zeroes of  $\beta_v$ . For  $\epsilon > 0$ , there is a nontrivial infrared stable fixed point

$$v_* = \frac{3}{4}(\epsilon - 0.141\epsilon^2 + \mathcal{O}(\epsilon^3)) . \quad (38)$$

The other fixed point  $v_* = 0$  being Gaussian is stable only if  $\epsilon < 0$ .

From the nontrivial fixed point value  $\zeta(v_*)$  we define the anomaly exponent  $\eta := -\frac{1}{2}\zeta(v_*)$  that is to two-loop order

$$\eta = \frac{1}{4}\epsilon(1 - 0.302 \frac{\epsilon}{9} + \mathcal{O}(\epsilon^2)) . \quad (39)$$

At the fixed point the solution of the second flow equation of equation (35) is

$$\bar{\rho}(l) = \rho l^{-2\eta} . \quad (40)$$

The results found for the vertex functions in the quasi-static model can be directly transferred into the dynamic model because the time scale  $\lambda$  needs no renormalization.

The longitudinal length scale transformation according to equation (21), dimensional analysis and the renormalization group equation are now combined to derive the asymptotic critical scaling form of the vertex functions in the dynamic model at the transverse phase transition

$$\Gamma_{\tilde{n},n}(\{q_\parallel, \mathbf{q}_\perp, \omega\}, \tau_\perp, v_*, \lambda, \rho, \mu) = l^{-\frac{1}{2}\eta(\tilde{n}+n-2)-\frac{1}{2}\tilde{n}(d+7)-\frac{1}{2}n(d-5)+d+5} \Gamma_{\tilde{n},n}\left(\left\{\frac{q_\parallel}{l^{2+\eta}}, \frac{\mathbf{q}_\perp}{l}, \frac{\omega}{l^4}\right\}, \frac{\tau_\perp}{l^2}, v_*, \lambda, \rho, \mu\right) \quad (41)$$

This equation implies that, below the upper critical dimension  $d_c = 9$ , anomalous scaling behaviour only occurs in the direction of the driving force and is completely characterized by the anomaly exponent  $\eta$  from (39) that is positive. These results are in analogy to what was found in the driven diffusive

systems investigated so far [4, 5, 7, 13].

To illustrate the importance of the positive anomaly exponent  $\eta$  we especially investigate the density response function  $\chi(\mathbf{q}, t)$  which is the Fourier transform of  $\Gamma_{1,1}^{-1}(\mathbf{q}, \omega)$ . Choosing the flow parameter  $l = \omega^{\frac{1}{4}} \ll 1$ , we derive the scaling form of the density response function  $\chi(\mathbf{q}, t) := \langle s(\mathbf{q}, t) \tilde{s}(-\mathbf{q}, 0) \rangle$  from equation (41):

$$\chi(\mathbf{q}, t) = f\left(q_{\parallel}^2 t^{1+\frac{1}{2}\eta}, q_{\perp}^2 t^{\frac{1}{2}}\right). \quad (42)$$

From that we conclude that for long times typical longitudinal length-squares scale with time as

$$\langle r_{\parallel}^2 \rangle \sim t^{1+\frac{1}{2}\eta}. \quad (43)$$

The positivity of  $\eta = \frac{1}{4}\epsilon(1 - 0.302 \frac{\epsilon}{9} + \mathcal{O}(\epsilon^2))$  means that in systems with spatial dimensions  $d < d_c = 9$  fluctuations spread faster than diffusively in the driving force direction. This superdiffusion was also observed in all driven diffusive systems analyzed up to now [4, 5, 7, 13].

A comparison with the corresponding model for the transverse phase transition without quenched disorder, having an upper critical dimension  $d_c = 5$ , shows that the phenomenon of superdiffusion occurs here over a much greater dimensional range. As the system without quenched disorder behaves normally diffusive for  $d > 5$  it follows that quenched disorder is the reason for superdiffusion in the dimensional interval  $5 < d < 9$ .

The analogous comparison of the models with and without disorder for the noncritical region [4, 7] came to an analogous result.

Another consequence from the scaling form of the density response function is that typical transverse length-squares scale as  $\langle r_{\perp}^2 \rangle \sim t^{\frac{1}{2}}$  for long times, i.e. subdiffusively. This behaviour corresponds to the naive dynamical exponent  $z = 4$  in model B (in the nomenclature of Halperin and Hohenberg [23]) and has been expected, for the system here is critical with respect to the transverse directions and no renormalizations are necessary in this subspace. The extrapolation of the anomaly-exponent  $\eta$  into low dimensions is difficult in view of the high upper critical dimension  $d_c = 9$ . Naively, we can simply set  $\epsilon = d_c - d = 6$  in Equation (39) to predict  $\eta$  f.e. in a 3-dimensional system, resulting in an estimate

$$\eta(d=3) = 1.20. \quad (44)$$

Although  $\epsilon$  has been considered as small quantity the two loop-correction with respect to the one-loop result is merely 20%, even at  $\epsilon = 6$ . Due

to these small corrections we expect that equation (39), even though it is strictly valid only near  $d_c = 9$ , produces good approximations for  $\eta$  also in low dimensions.

### 3.2 Random Potential With Equally High Potential Mountains

This model is analyzed in analogy to the model with unsymmetric random potential of the last section. The quenched disorder according to Equation (13) resulting from the random potential with equally high potential mountains leads, in analogy to Equation (15), to the dynamic functional

$$\mathcal{J}[s, \tilde{s}] = \int d^d r \left\{ \int dt [\tilde{s} (\dot{s} + \lambda(\Delta_\perp(\kappa_\perp \Delta_\perp - \tau_\perp) + \rho \Delta_\parallel(\kappa_\parallel \Delta_\parallel - \tau_\parallel) + \kappa \Delta_\perp \Delta_\parallel) s) + \frac{1}{2} \lambda g (\nabla_\parallel \tilde{s}) s^2] - \alpha \left[ \lambda \int dt \Delta_\perp \tilde{s} \right]^2 - \sigma \left[ \lambda \int dt \nabla_\parallel \tilde{s} \right]^2 \right\}, \quad (45)$$

that still contains irrelevant terms to be eliminated.

Transverse and longitudinal lengths scale as before  $r_\perp \sim \mu^{-1}$ ,  $r_\parallel \sim \mu^{-2}$ . Since the dynamic functional is dimensionless the dimension of fields and coupling constants are

$$\begin{array}{lll} \lambda t \sim \mu^{-4} & s \sim \mu^{\frac{d-3}{2}} & \tilde{s} \sim \mu^{\frac{d+5}{2}} \\ \kappa_\parallel \sim \mu^{-4} & \kappa \sim \mu^{-2} & \sigma \sim \mu^0 \\ \alpha \sim \mu^0 & g \sim \mu^{\frac{7-d}{2}} & . \end{array} \quad (46)$$

Thus, the coupling constants  $\kappa_\parallel$  and  $\kappa$  are again irrelevant in the renormalization group sense, but  $\sigma$  is not. This signifies that in the given random potential both longitudinal and transverse noise are relevant. The dimension of the nonlinear coupling  $g$  shows that

$$d_c = 7 \quad (47)$$

is the upper critical dimension of this model. The finite  $\tau_\parallel$  and the transverse coupling constants  $\alpha$  and  $\kappa_\perp$  are again absorbed by a suitable scale change. Thus, the appropriate dynamic functional for the transverse phase transition in the given random potential is

$$\begin{aligned} \mathcal{J}[s, \tilde{s}] = \int d^d r \left\{ \int dt \left[ \tilde{s} \dot{s} + \lambda \tilde{s} (\Delta_\perp (\Delta_\perp - \tau_\perp) - \rho \Delta_\parallel) s + \frac{1}{2} \lambda g (\nabla_\parallel \tilde{s}) s^2 \right] \right. \\ \left. - \left[ \lambda \int dt \Delta_\perp \tilde{s} \right]^2 - \sigma \left[ \lambda \int dt \nabla_\parallel \tilde{s} \right]^2 \right\}. \end{aligned} \quad (48)$$



This dynamic functional exhibits the same symmetries as the one in the case of the unsymmetric random potential, except the longitudinal scale transformation, where here the parameter  $\sigma$  is additionally transformed according to  $\sigma \rightarrow \beta^2 \sigma$ . In addition to the parameter combination  $g^2 \rho^{-\frac{3}{2}}$ ,  $\sigma \rho^{-1}$  is also an invariant variable of this model and the perturbation expansion will be organized in powers of both variables.

Due to the quenched disorder, the Gaussian correlator is again time independent so that, for simplicity, we also here transform  $\mathcal{J}$  into a quasi-static Hamiltonian via (26) and (27)

$$\begin{aligned} \mathcal{H}[\varphi, \tilde{\varphi}] = \int d^d r \left\{ \tilde{\varphi}(\Delta_{\perp}(\Delta_{\perp} - \tau_{\perp}) - \rho \Delta_{\parallel})\varphi + \frac{1}{2}g(\nabla_{\parallel}\tilde{\varphi})\varphi^2 \right. \\ \left. + \tilde{\varphi}(-\Delta_{\perp}^2 + \sigma \Delta_{\parallel})\tilde{\varphi} \right\}. \end{aligned} \quad (49)$$

In comparison with the former model, the vertex and the Gaussian propagator remain the same (29), whereas the Gaussian correlator of the quasistatic model reads

$$C_{\mathbf{q}} = \frac{2(\mathbf{q}_{\perp}^4 + \sigma q_{\parallel}^2)}{[\mathbf{q}_{\perp}^2(\mathbf{q}_{\perp}^2 + \tau_{\perp}) + \rho q_{\parallel}^2]^2}. \quad (50)$$

By dimensional analysis taking into account the causality properties we find the vertex functions  $\Gamma_{1,1}$ ,  $\Gamma_{2,0}$ , and  $\Gamma_{1,2}$  primitively divergent. Neglecting higher orders in  $q$  and  $\epsilon = d_c - d$ , a one-loop calculation for these vertex functions, with dimensional regularization, results in

$$\begin{aligned} \mathring{\Gamma}_{1,1}(\mathbf{q}) &= \mathbf{q}_{\perp}^2(\mathbf{q}_{\perp}^2 + \tau_{\perp}) + \rho q_{\parallel}^2 + \frac{B_{\epsilon}}{\epsilon} \frac{\mathring{g}^2}{\rho^{\frac{1}{2}}} q_{\parallel}^2 \tau_{\perp}^{-\frac{\epsilon}{2}} \\ \mathring{\Gamma}_{2,0}(\mathbf{q}) &= -2\mathbf{q}_{\perp}^4 - 2\mathring{\sigma} q_{\parallel}^2 - \frac{1}{4} \frac{B_{\epsilon}}{\epsilon} \frac{\mathring{g}^2}{\rho^{\frac{1}{2}}} q_{\parallel}^2 \tau_{\perp}^{-\frac{\epsilon}{2}} \left( 5 + 2\frac{\mathring{\sigma}}{\rho} + \left( \frac{\mathring{\sigma}}{\rho} \right)^2 \right) \\ \mathring{\Gamma}_{1,2}(\mathbf{q}) &= i\mathring{g}q_{\parallel} - i\frac{1}{4} \frac{B_{\epsilon}}{\epsilon} \frac{\mathring{g}^3}{\rho^{\frac{3}{2}}} q_{\parallel} \tau_{\perp}^{-\frac{\epsilon}{2}} \left( 1 + \frac{\mathring{\sigma}}{\rho} \right), \end{aligned} \quad (51)$$

where

$$B_{\epsilon} = \frac{1}{(2\pi)^d} \mathcal{O}_{d-1} \Gamma(1 + \frac{\epsilon}{2}) \Gamma(\frac{3-\epsilon}{2}) \Gamma(\frac{1}{2}) \quad (52)$$

is a suitably chosen  $\epsilon$ -dependent factor. Notice that although not performed a two-loop calculation could here also be done with the method described in

the Appendix.

The primitive divergences are absorbed in the redefinition of the parameters

$$\mathring{\rho} = Z_\rho \rho, \quad \mathring{\sigma} = Z_\sigma \sigma, \quad \mathring{g} = \mu^{\frac{\epsilon}{2}} Z_u u. \quad (53)$$

In comparison to the latter model the coupling constant  $\mathring{\sigma}$  has additionally to be renormalized. From Equation (51) we easily obtain the  $Z$ -Factors in minimal subtraction

$$\begin{aligned} Z_\rho &= 1 - \frac{v}{\epsilon} + \mathcal{O}(v^2) \\ Z_\sigma &= 1 - \frac{1}{8} \frac{v}{\epsilon} \frac{1}{w} (5 + 2w + w^2) + \mathcal{O}(v^2) \\ Z_u &= 1 + \frac{1}{4} \frac{v}{\epsilon} (1 + w) + \mathcal{O}(v^2), \end{aligned} \quad (54)$$

expressed as functions of the dimensionless renormalized parameters  $v := B_\epsilon u^2 \rho^{-\frac{3}{2}}$  and  $w := \sigma \rho^{-1}$  that are invariant under the longitudinal scale transformation.

In analogy to the former model we obtain the renormalization group equation

$$\left[ \beta_v \frac{\partial}{\partial v} + \beta_w \frac{\partial}{\partial w} + \rho \zeta \frac{\partial}{\partial \rho} + \mu \frac{\partial}{\partial \mu} \right] \Gamma_{\tilde{n},n}(\{q_\parallel, \mathbf{q}_\perp\}, \tau_\perp, v, w, \rho, \mu) = 0 \quad (55)$$

with the parameter functions depending on  $v$  and  $w$

$$\begin{aligned} \beta_v &:= \left. \mu \frac{\partial v}{\partial \mu} \right|_o = -v \left[ \epsilon - \frac{1}{2} v (4 + w) + \mathcal{O}(v^2) \right] \\ \beta_w &:= \left. \mu \frac{\partial w}{\partial \mu} \right|_o = -\frac{1}{8} v [5 - 6w + w^2] + \mathcal{O}(v^2) \\ \zeta &:= \left. \mu \frac{\partial \ln \rho}{\partial \mu} \right|_o = -v + \mathcal{O}(v^2). \end{aligned} \quad (56)$$

The associated characteristics are defined by

$$\begin{aligned} l \frac{d}{dl} \bar{v}(l) &= \beta_v(\bar{v}(l), \bar{w}(l)) & l \frac{d}{dl} \ln \bar{\rho}(l) &= \zeta(\bar{v}(l), \bar{w}(l)) \\ l \frac{d}{dl} \bar{w}(l) &= \beta_w(\bar{v}(l), \bar{w}(l)) & l \frac{d}{dl} \bar{\mu}(l) &= \bar{\mu}(l) \end{aligned} \quad (57)$$

with the initial condition  $\bar{w}(l = 1) = w$  and the initial conditions from Equation (36). In the scaling limit  $l \ll 1$ ,  $\bar{v}(l)$  and  $\bar{w}(l)$  flow to an infrared

stable fixed point  $(v_*, w_*)$  given by the zeroes of  $\beta_v$  and  $\beta_w$  with a positive gradient. The zeroes of  $\beta_w$  in this order are

$$w_1 = 1 \quad w_2 = 5, \quad (58)$$

and those of  $\beta_v$

$$v_1 = 0 \quad v_2 = \frac{2\epsilon}{4+w}. \quad (59)$$

This yields the infrared stable fixed point

$$w_* = 1 + \mathcal{O}(\epsilon) \quad v_* = \frac{2}{5}\epsilon + \mathcal{O}(\epsilon^2). \quad (60)$$

The domain of attraction of this fixed point can easily be recognized as

$$v > 0 \quad w < 5 + \mathcal{O}(\epsilon). \quad (61)$$

In the case  $w > 5 + \mathcal{O}(\epsilon)$  the critical behaviour of the system is dominated by the degenerate fixed point

$$w_* = \infty \quad v_* = 0. \quad (62)$$

Concerning this degenerate fixed point we remark the following:

i) For  $w \rightarrow \infty$  the transverse noise vanishes in comparison to the longitudinal one. This can be seen easily by substituting  $\rho q_{\parallel}^2 \rightarrow q_{\parallel}^2$  and extracting  $\sigma \rho^{-1} = w$  from the correlator. Then the remaining coefficient of the longitudinal part in the numerator of the correlator is 1, the coefficient of the transverse part is  $w^{-1}$ . At the degenerate fixed point, this system here behaves as the model with a random potential with equally deep potential valleys and whose noise is therefore given by Equation (14). This model is analyzed in the next section, but we anticipate some results concerning the degenerate fixed point. According to Eq. (76) the degenerate fixed point possesses a finite fixed point value  $(v \cdot w)_* = \frac{8}{3}\epsilon + \mathcal{O}(\epsilon^2)$ . Although the deviations from normal diffusive behaviour only appear in order two-loop, the positive  $\eta$  from Eq. (77) demonstrates the system to be also superdiffusive at the degenerate fixed point.

ii) Both a “normal” and a degenerate fixed point are also observed in the noncritical model with quenched disorder [7]. While here at the transverse phase transition the situation of two fixed points appears in the random potential with equally high mountains and the degenerate fixed point is described by the model with the random potential with equally deep valleys,

in the noncritical region, however, the situation of a normal and a degenerate fixed point occurs in the model with unsymmetric random potential and the degenerate fixed point is described by both the model with equally high mountains and equally deep valleys, for these latter models are identical in the noncritical region.

Now we proceed to investigate the normal fixed point (60). For this fixed point the anomaly–exponent reads

$$\eta = \frac{1}{5}\epsilon + \mathcal{O}(\epsilon^2) . \quad (63)$$

At the fixed point, the second characteristic has the form

$$\bar{\rho}(l) = \rho l^{-2\eta} \quad (64)$$

in analogy to Equation (40).

Returning to the dynamic model and again exploiting the renormalization group equation at the fixed point, dimensional analysis, and the invariant scale transformation we obtain the universal scaling behaviour of the vertex functions in the asymptotic limit

$$\begin{aligned} \Gamma_{\tilde{n},n}(\{q_{\parallel}, \mathbf{q}_{\perp}, \omega\}, \tau_{\perp}, v_*, w_*, \lambda, \rho, \mu) = \\ l^{-\frac{1}{2}\eta(\tilde{n}+n-2)-\frac{1}{2}\tilde{n}(d+5)-\frac{1}{2}n(d-3)+d+5} \Gamma_{\tilde{n},n}\left(\left\{\frac{q_{\parallel}}{l^{2+\eta}}, \frac{\mathbf{q}_{\perp}}{l}, \frac{\omega}{l^4}\right\}, \frac{\tau_{\perp}}{l^2}, v_*, w_*, \lambda, \rho, \mu\right) . \end{aligned} \quad (65)$$

Thus, only longitudinal lengths scale anomalously below the upper critical dimension  $d_c = 7$ . From this equation we derive the scaling form of the density response function

$$\chi(\mathbf{q}, t) = f\left(q_{\parallel}^2 t^{1+\frac{1}{2}\eta}, q_{\perp}^2 t^{\frac{1}{2}}\right) \quad (66)$$

which coincides with the form found for the preceding model. The positivity of  $\eta = \frac{1}{5}\epsilon + \mathcal{O}(\epsilon^2)$  signifies superdiffusive behaviour below  $d_c = 7$ . A comparison with the corresponding model without quenched disorder again shows the quenched disorder to be the reason for the enhanced spread of fluctuations in the driving force direction in a dimensional interval that is here, however,  $5 < d < 7$ .

A straightforward extrapolation of the anomaly–exponent into three dimensions by setting  $\epsilon = 4$  into the one-loop result gives the approximate value

$$\eta(d=3) = \frac{4}{5} . \quad (67)$$

This numerical value is very distinct from the one-loop and two-loop values for  $\eta$  in the model with unsymmetric random potential.

We now discuss the case that the transverse noise term with  $\gamma \neq 0$  of Equation (15) is generated by coarse graining even in this symmetric random potential. Then an additional scaling variable  $\gamma/l^\phi$  arises in (65). The crossover exponent is here  $\phi = 2$  and it simply reflects the naive dimension of the coupling constant  $\gamma$ , because  $\gamma$  itself is invariant under the longitudinal scale transformation and for dimensional reasons the transverse noise term with  $\gamma \neq 0$  needs no additional renormalization. Since  $\gamma$  is a relevant variable, for  $\gamma \neq 0$  the system eventually flows to the fixed point of the model with unsymmetric random potential.

### 3.3 Random Potential With Equally Deep Potential Valleys

Having no transverse noise according to Equation (14) this model is formally obtained from the model with random potential with equally high mountains by setting the transverse noise coefficient  $\alpha = 0$ . Then the relevant dynamic functional is here

$$\mathcal{J}[s, \tilde{s}] = \int d^d r \left\{ \int dt \left[ \tilde{s} \dot{s} + \lambda \tilde{s} (\Delta_\perp (\Delta_\perp - \tau_\perp) - \rho \Delta_\parallel) s + \frac{1}{2} \lambda g (\nabla_\parallel \tilde{s}) s^2 \right] - \sigma \left[ \lambda \int dt \nabla_\parallel \tilde{s} \right]^2 \right\}. \quad (68)$$

The dimensions of lengths, fields, and coupling constants as well as the upper critical dimension  $d_c = 7$  are as in the latter model. The symmetry properties of this dynamic functional are the same as in both preceding models with the exception of the invariant scale transformation. The lack of the transverse noise term has the consequence that the dynamic functional is invariant under a scale transformation depending on two parameters

$$\begin{aligned} r_\parallel &\rightarrow \beta r_\parallel & r_\perp &\rightarrow r_\perp & (69) \\ \tilde{s} &\rightarrow \alpha \tilde{s} & s &\rightarrow \alpha^{-1} \beta^{-1} s \\ \rho &\rightarrow \beta^2 \rho & g &\rightarrow \alpha \beta^2 g & \sigma &\rightarrow \alpha^{-2} \beta \sigma. \end{aligned}$$

Therefore, the combination of coupling constants  $g^2 \sigma \rho^{-\frac{5}{2}}$  is the appropriate invariant variable in this model and is exactly the product of the variables

being invariant each in the latter model, but not here.

Because of the quenched disorder we again use the transformation to a quasi-static Hamiltonian

$$\mathcal{H}[\varphi, \tilde{\varphi}] = \int d^d r \left\{ \tilde{\varphi}(\Delta_{\perp}(\Delta_{\perp} - \tau_{\perp}) - \rho \Delta_{\parallel})\varphi + \frac{1}{2}g(\nabla_{\parallel}\tilde{\varphi})\varphi^2 + \sigma\tilde{\varphi}\Delta_{\parallel}\tilde{\varphi} \right\} . \quad (70)$$

Vertex and Gaussian propagator are the same as in both preceding models, whereas the Gaussian correlator reads

$$C_{\mathbf{q}} = \frac{2\sigma q_{\parallel}^2}{[\mathbf{q}_{\perp}^2(\mathbf{q}_{\perp}^2 + \tau_{\perp}) + \rho q_{\parallel}^2]^2} . \quad (71)$$

As in the previous model  $\Gamma_{1,1}$ ,  $\Gamma_{2,0}$ , and  $\Gamma_{1,2}$  are primitively divergent. We have computed them in the lowest nonvanishing order, i.e. we have performed a one-loop calculation for  $\Gamma_{2,0}$  and  $\Gamma_{1,2}$  and a two-loop calculation for  $\Gamma_{1,1}$ . The two-loop calculation involves similar integrals as in the model with unsymmetric random potential and has also been performed with the help of inverse Mellin transformation (cf. Appendix).

In dimensional regularization we obtain the primitively divergent vertex functions, up to higher order terms in  $q$  and  $\epsilon = d_c - d$

$$\begin{aligned} \mathring{\Gamma}_{1,1}(\mathbf{q}) &= \mathbf{q}_{\perp}^2(\mathbf{q}_{\perp}^2 + \tau_{\perp}) + \rho q_{\parallel}^2 - 4 \frac{B_{\epsilon}^2}{\epsilon^2} \frac{\mathring{g}^4 \mathring{\sigma}^2}{\rho^4} q_{\parallel}^2 \tau_{\perp}^{-\epsilon} (0 - 0.001799\epsilon) \quad (72) \\ \mathring{\Gamma}_{2,0}(\mathbf{q}) &= -2\mathring{\sigma} q_{\parallel}^2 - \frac{1}{4} \frac{B_{\epsilon}}{\epsilon} \frac{\mathring{g}^2 \mathring{\sigma}^2}{\rho^{\frac{5}{2}}} q_{\parallel}^2 \tau_{\perp}^{-\frac{\epsilon}{2}} \\ \mathring{\Gamma}_{1,2}(\mathbf{q}) &= i\mathring{g} q_{\parallel} - i \frac{1}{4} \frac{B_{\epsilon}}{\epsilon} \frac{\mathring{g}^3 \mathring{\sigma}}{\rho^{\frac{5}{2}}} q_{\parallel} \tau_{\perp}^{-\frac{\epsilon}{2}} , \end{aligned}$$

where  $B_{\epsilon}$  is defined by Equation (52). The same redefinition of the coupling constants as in Equation (53) absorbs these divergences and yields in minimal subtraction

$$\begin{aligned} Z_{\rho} &= 1 - 0.007196 \frac{v^2}{\epsilon} + \mathcal{O}(v^3) \\ Z_{\sigma} &= 1 - \frac{1}{8} \frac{v}{\epsilon} + \mathcal{O}(v^2) \\ Z_u &= 1 + \frac{1}{4} \frac{v}{\epsilon} + \mathcal{O}(v^2) , \end{aligned} \quad (73)$$

where  $v := B_\epsilon u^2 \sigma \rho^{-\frac{5}{2}}$  is the dimensionless renormalized variable of the model. This variable is invariant under the longitudinal scale transformation (Eq. (69)) and is the product of  $v$  and  $w$  in the latter model, but it will here merely be denoted by  $v$  for simplicity.

The renormalization group equation reads

$$\left[ \beta_v \frac{\partial}{\partial v} + \rho \zeta_\rho \frac{\partial}{\partial \rho} + \sigma \zeta_\sigma \frac{\partial}{\partial \sigma} + \mu \frac{\partial}{\partial \mu} \right] \Gamma_{\tilde{n},n}(\{q_\parallel, \mathbf{q}_\perp\}, \tau_\perp, v, \rho, \sigma, \mu) = 0 \quad (74)$$

with the Wilson parameter functions

$$\begin{aligned} \beta_v &:= \left. \mu \frac{\partial v}{\partial \mu} \right|_o = -v \left[ \epsilon - \frac{3}{8}v + \mathcal{O}(v^2) \right] \\ \zeta_\sigma &:= \left. \mu \frac{\partial \ln \sigma}{\partial \mu} \right|_o = -\frac{1}{8}v + \mathcal{O}(v^2) \\ \zeta_\rho &:= \left. \mu \frac{\partial \ln \rho}{\partial \mu} \right|_o = -0.01439v^2 + \mathcal{O}(v^3) \end{aligned} \quad (75)$$

only depending on  $v$ .

The infrared stable fixed point, being a zero of  $\beta_v$ , is found at

$$v_* = \frac{8}{3}\epsilon + \mathcal{O}(\epsilon^2) . \quad (76)$$

Hence we obtain the anomaly-exponent

$$\eta = 0.0512\epsilon^2 + \mathcal{O}(\epsilon^3) . \quad (77)$$

The characteristics of the renormalization group equation are defined by Equation (35) and an additional equation for  $\bar{\sigma}(l)$  that has the same structure as the equation for  $\bar{\rho}(l)$ . At the fixed point the solutions for these flow equations read

$$\bar{\rho}(l) = \rho l^{-2\eta} \quad \bar{\sigma}(l) = \sigma l^{\zeta_{\sigma*}} , \quad (78)$$

where

$$\zeta_{\sigma*} := \zeta_\sigma(v_*) = -\frac{1}{3}\epsilon + \mathcal{O}(\epsilon^2) . \quad (79)$$

Returning to the dynamic model and combining the renormalization group equation at the fixed point, dimensional analysis, and the invariant longitudinal scale transformation we obtain the universal scaling behaviour of the

vertex functions in the asymptotic limit

$$\Gamma_{\tilde{n},n}(\{q_{\parallel}, \mathbf{q}_{\perp}, \omega\}, \tau_{\perp}, v_*, \lambda, \rho, \sigma, \mu) = l^{-\eta(-1+\frac{3}{2}n-\frac{1}{2}\tilde{n})+\frac{1}{2}\zeta_{\sigma*}(\tilde{n}-n)-\frac{1}{2}\tilde{n}(d+5)-\frac{1}{2}n(d-3)+d+5} \cdot \Gamma_{\tilde{n},n}\left(\left\{\frac{q_{\parallel}}{l^{2+\eta}}, \frac{\mathbf{q}_{\perp}}{l}, \frac{\omega}{l^4}\right\}, \frac{\tau_{\perp}}{l^2}, v_*, \lambda, \rho, \sigma, \mu\right) \quad (80)$$

We again see that only longitudinal lengths scale anomalously. In contrast to both preceding models there is here an additional exponent  $\zeta_{\sigma*}$  appearing in the global  $l$ -factor. As this exponent is cancelled for  $\Gamma_{1,1}$ , the density response function nevertheless has the scaling form

$$\chi(\mathbf{q}, t) = f\left(q_{\parallel}^2 t^{1+\frac{1}{2}\eta}, q_{\perp}^2 t^{\frac{1}{2}}\right) \quad (81)$$

in analogy to both preceding models. As the anomaly-exponent  $\eta = 0.0512\epsilon^2 + \mathcal{O}(\epsilon^3)$  is positive and the upper critical dimension  $d_c = 7$  is the same as in the preceding model, all statements concerning superdiffusion and speeding-up of fluctuations by quenched disorder are here also valid.

The straightforward extrapolation of  $\eta$  from  $d_c = 7$  to  $d = 3$  by setting  $\epsilon = 4$  produces the approximative value

$$\eta(d=3) = 0.82. \quad (82)$$

This numerical value is close to the one-loop value for  $\eta$  in  $d = 3$  in the model with random potential with equally high mountains, but is very far from the one-loop and two-loop values in the model with unsymmetric random potential.

We now investigate the possibility that even in this symmetric random potential transverse noise terms are produced by coarse graining. First, we consider the case that transverse noise proportional to  $\alpha \int d^d r [\lambda \int dt \Delta_{\perp} \tilde{s}]^2$  is generated. Then we are in the situation of the preceding model. If  $\alpha$  is small the system is in the region of attraction of the degenerate fixed point discussed in this section. This implies that the transverse noise vanishes under the renormalization flow and the results of this section remain valid.

Second, if transverse noise proportional to  $\gamma \int d^d r [\lambda \int dt \nabla_{\perp} \tilde{s}]^2$  is produced, an additional scaling variable  $\gamma/l^{\phi}$  arises in (80). Due to dimensional reasons, this relevant operator needs no additional renormalization. The invariant scale transformation according to Equation (69) implies  $\gamma \rightarrow \beta^{-1}\alpha^{-2}\gamma$ . Thus, the crossover exponent is related to the exponents  $\eta$  and  $\zeta_{\sigma*}$  by  $\phi = 2 + 2\eta - \zeta_{\sigma*}$ . For  $\gamma \neq 0$  the system eventually flows to the fixed point of the model with unsymmetric random potential, because  $\gamma$  is a relevant variable.



## 4 Longitudinal Phase Transition

The three different realizations of the random potential I–III described in Section 2 converge to a single model in the region of the longitudinal phase transition as is sketched in the following.

For the three realizations of the random potential the dynamic functional still containing many irrelevant terms is given by Eq. (15) and by Eq. (45) with  $\alpha \neq 0$  and  $\alpha = 0$ , respectively. The longitudinal phase transition is characterized by  $\tau_{\parallel} \rightarrow 0$  and finite  $\tau_{\perp}$ . The external scale  $\mu^2$  here measures small  $\tau_{\parallel}$ . Comparing the leading gradient terms in driving force direction ( $\sim \lambda \tilde{s} \rho \Delta_{\parallel} \kappa_{\parallel} \Delta_{\parallel} s$ ) and transverse direction ( $\sim \lambda \tilde{s} \tau_{\perp} \Delta_{\perp} s$ ) we find for length scales

$$r_{\parallel} \sim \mu^{-1} \quad r_{\perp} \sim \mu^{-2}. \quad (83)$$

As the dynamic functional is dimensionless the coupling constants of the transverse noise scale as  $\gamma \sim \mu^{-2}$ ,  $\alpha \sim \mu^{-6}$ , i.e., only the longitudinal noise is relevant. Hence, only a single model is required to describe the longitudinal phase transition, independent of the kind of the random potential. Further, the dimensions of fields and the other coupling constants are

$$\begin{aligned} \lambda t &\sim \mu^{-4} & s &\sim \mu^{d-\frac{7}{2}} & \tilde{s} &\sim \mu^{d+\frac{5}{2}} \\ \kappa_{\perp} &\sim \mu^{-4} & \kappa &\sim \mu^{-2} & \sigma &\sim \mu^0 \\ g &\sim \mu^{\frac{13}{2}-d}, \end{aligned} \quad (84)$$

indicating that  $\kappa_{\perp}$  and  $\kappa$  are irrelevant and that

$$d_c = 6.5 \quad (85)$$

is the upper critical dimension of this model.

After a suitable scale change of fields and lengths the relevant dynamic functional for the longitudinal phase transition is

$$\begin{aligned} \mathcal{J}[s, \tilde{s}] = \int d^d r \left\{ \int dt \left[ \tilde{s} \dot{s} + \lambda \tilde{s} (-\Delta_{\perp} + \rho \Delta_{\parallel} (\rho \Delta_{\parallel} - \tau_{\parallel})) s + \frac{1}{2} \lambda g (\nabla_{\parallel} \tilde{s}) s^2 \right] \right. \\ \left. - \sigma \left[ \lambda \int dt \nabla_{\parallel} \tilde{s} \right]^2 \right\}. \end{aligned} \quad (86)$$

The symmetry properties are the same as in the last model of Section 3 inclusively the invariant longitudinal scale transformation, because transverse noise exists in neither model. As a consequence  $g^2 \sigma \rho^{-\frac{5}{2}}$  is the appropriate

invariant variable of this model.

Due to the quenched disorder, we transform to a quasistatic Hamiltonian

$$\mathcal{H}[\varphi, \tilde{\varphi}] = \int d^d r \left\{ \tilde{\varphi}(-\Delta_{\perp} + \rho\Delta_{\parallel}(\rho\Delta_{\parallel} - \tau_{\parallel}))\varphi + \frac{1}{2}g(\nabla_{\parallel}\tilde{\varphi})\varphi^2 + \sigma\tilde{\varphi}\Delta_{\parallel}\tilde{\varphi} \right\}. \quad (87)$$

From this equation we directly read off the elements of perturbation theory, i.e., the vertex  $-igq_{\parallel}$  and the Gaussian propagator and correlator

$$\begin{aligned} G_{\mathbf{q}} &= \frac{1}{\mathbf{q}_{\perp}^2 + \rho q_{\parallel}^2(\rho q_{\parallel}^2 + \tau_{\parallel})} \\ C_{\mathbf{q}} &= \frac{2\sigma q_{\parallel}^2}{[\mathbf{q}_{\perp}^2 + \rho q_{\parallel}^2(\rho q_{\parallel}^2 + \tau_{\parallel})]^2}. \end{aligned} \quad (88)$$

The vertex functions  $\Gamma_{1,1}$ ,  $\Gamma_{2,0}$ , and  $\Gamma_{1,2}$  are primitively divergent. The singular parts of  $\Gamma_{1,1}$  are proportional to  $q_{\parallel}^4$  and  $q_{\parallel}^2$ , the singular parts of  $\Gamma_{2,0}$  and  $\Gamma_{1,2}$  are proportional to  $q_{\parallel}^2$  and  $q_{\parallel}$ , respectively.

In a one-loop calculation we obtain the primitively divergent regularized vertex functions in bare quantities up to higher orders in  $q$  and  $\epsilon = d_c - d$

$$\begin{aligned} \mathring{\Gamma}_{1,1}(\mathbf{q}) &= \mathbf{q}_{\perp}^2 + \mathring{\rho}q_{\parallel}^2(\mathring{\rho}q_{\parallel}^2 + \mathring{\tau}_{\parallel}) + \frac{C_{\epsilon}}{\epsilon} \frac{\mathring{g}^2 \mathring{\sigma}}{\mathring{\rho}^{\frac{3}{2}}} q_{\parallel}^2 \mathring{\tau}_{\parallel}^{-\epsilon} \left( \frac{1}{6} \mathring{\rho}q_{\parallel}^2 + 0 \cdot \mathring{\tau}_{\parallel} \right) \\ \mathring{\Gamma}_{2,0}(\mathbf{q}) &= -2\mathring{\sigma}q_{\parallel}^2 - \frac{1}{6} \frac{C_{\epsilon}}{\epsilon} \frac{\mathring{g}^2 \mathring{\sigma}^2}{\mathring{\rho}^{\frac{5}{2}}} q_{\parallel}^2 \mathring{\tau}_{\parallel}^{-\epsilon} \\ \mathring{\Gamma}_{1,2}(\mathbf{q}) &= i\mathring{g}q_{\parallel} - i\frac{1}{6} \frac{C_{\epsilon}}{\epsilon} \frac{\mathring{g}^3 \mathring{\sigma}}{\mathring{\rho}^{\frac{5}{2}}} q_{\parallel} \mathring{\tau}_{\parallel}^{-\epsilon}, \end{aligned} \quad (89)$$

where

$$C_{\epsilon} = \frac{1}{(2\pi)^d} \mathcal{O}_{d-1} \Gamma(1+\epsilon) \Gamma\left(\frac{11-2\epsilon}{4}\right) \Gamma\left(\frac{5-2\epsilon}{4}\right) \quad (90)$$

is a suitably chosen  $\epsilon$ -dependent factor. These divergences are absorbed in the redefinition of the coupling constants

$$\mathring{\rho} = Z_{\rho}\rho \quad \mathring{\tau}_{\parallel} = Z_{\tau_{\parallel}}\tau_{\parallel} \quad \mathring{\sigma} = Z_{\sigma}\sigma \quad \mathring{g} = \mu^{\epsilon}Z_u u. \quad (91)$$

In minimal subtraction we obtain the  $Z$ -factors as a function of the dimensionless renormalized invariant variable  $v := C_{\epsilon}u^2\sigma\rho^{-\frac{5}{2}}$

$$Z_{\rho} = 1 - \frac{1}{12} \frac{v}{\epsilon} + \mathcal{O}(v^2) \quad (92)$$

$$\begin{aligned}
Z_{\tau_{\parallel}} &= 1 + \frac{1}{12} \frac{v}{\epsilon} + \mathcal{O}(v^2) \\
Z_{\sigma} &= 1 - \frac{1}{12} \frac{v}{\epsilon} + \mathcal{O}(v^2) \\
Z_u &= 1 + \frac{1}{6} \frac{v}{\epsilon} + \mathcal{O}(v^2) .
\end{aligned}$$

Here, the renormalization group equation is of the form

$$\left[ \beta_v \frac{\partial}{\partial v} + \rho \zeta_{\rho} \frac{\partial}{\partial \rho} + \sigma \zeta_{\sigma} \frac{\partial}{\partial \sigma} + \kappa \tau_{\parallel} \frac{\partial}{\partial \tau_{\parallel}} + \mu \frac{\partial}{\partial \mu} \right] \Gamma_{\tilde{n},n}(\{q_{\parallel}, \mathbf{q}_{\perp}\}, \tau_{\parallel}, v, \rho, \sigma, \mu) = 0 \quad (93)$$

with the Wilson functions

$$\begin{aligned}
\beta_v &:= \mu \frac{\partial v}{\partial \mu} \Big|_o = -2v \left[ \epsilon - \frac{11}{24} v + \mathcal{O}(v^2) \right] \\
\zeta_{\sigma} &:= \mu \frac{\partial \ln \sigma}{\partial \mu} \Big|_o = -\frac{1}{6} v + \mathcal{O}(v^2) \\
\zeta_{\rho} &:= \mu \frac{\partial \ln \rho}{\partial \mu} \Big|_o = -\frac{1}{6} v + \mathcal{O}(v^2) \\
\kappa &:= \mu \frac{\partial \ln \tau_{\parallel}}{\partial \mu} \Big|_o = \frac{1}{6} v + \mathcal{O}(v^2) .
\end{aligned} \quad (94)$$

In addition to the flow equations for  $\bar{v}(l)$ ,  $\bar{\rho}(l)$ ,  $\bar{\sigma}(l)$ , and  $\bar{\mu}(l)$  being of the same form as in the preceding model there is a flow equation for  $\bar{\tau}_{\parallel}(l)$  that reads

$$\frac{d}{dl} \ln \bar{\tau}_{\parallel}(l) = \kappa(\bar{v}(l)) . \quad (95)$$

In the scaling limit  $l \ll 1$  that corresponds to the relations

$$\left| \frac{q_{\parallel}}{\mu} \right| \ll 1 \quad \left| \frac{\mathbf{q}_{\perp}}{\mu^2} \right| \ll 1 \quad \left| \frac{\tau_{\parallel}}{\mu^2} \right| \ll 1 \quad (96)$$

$\bar{v}(l)$  flows to an infrared stable fixed point  $v_*$  which is directly obtained as a zero of  $\beta_v$

$$v_* = \frac{24}{11} \epsilon + \mathcal{O}(\epsilon^2) . \quad (97)$$

At the fixed point the solutions of the flow equations are given by Equation (78) and by  $\bar{\tau}_{\parallel}(l) = \tau_{\parallel} l^{\kappa_*}$  with  $\kappa_* := \kappa(v_*)$ . Inserting the fixed point value

for  $v_*$  into  $\zeta_\rho$  we find the anomaly-exponent

$$\eta = \frac{2}{11}\epsilon + \mathcal{O}(\epsilon^2) . \quad (98)$$

The fixed point values of the other parameter functions are

$$\zeta_{\sigma*} = -\frac{4}{11}\epsilon + \mathcal{O}(\epsilon^2) \quad \kappa_* = \frac{4}{11}\epsilon + \mathcal{O}(\epsilon^2) . \quad (99)$$

Returning to the dynamic model and combining the solutions of the renormalization group equation at the fixed point with a dimensional analysis and the invariant scale transformation we finally arrive at the universal scaling behaviour of the vertex functions at the longitudinal phase transition

$$\begin{aligned} \Gamma_{\tilde{n},n}(\{q_{\parallel}, \mathbf{q}_{\perp}, \omega\}, \tau_{\parallel}, v_*, \lambda, \rho, \sigma, \mu) = \\ l^{-\eta(-1+\frac{3}{2}n-\frac{1}{2}\tilde{n})+\frac{1}{2}\zeta_{\sigma*}(\tilde{n}-n)-\frac{1}{2}\tilde{n}(2d+5)-\frac{1}{2}n(2d-7)+2d+3} \\ \cdot \Gamma_{\tilde{n},n}\left(\left\{\frac{q_{\parallel}}{l^{1+\eta}}, \frac{\mathbf{q}_{\perp}}{l^2}, \frac{\omega}{l^4}\right\}, \frac{\tau_{\parallel}}{l^{2-\kappa_*}}, v_*, \lambda, \rho, \sigma, \mu\right) \end{aligned} \quad (100)$$

In addition to longitudinal lengths the critical parameter  $\tau_{\parallel}$  also exhibits anomalous scaling behaviour. In analogy to the models in Section 3 we derive the scaling form of the density response function

$$\chi(\mathbf{q}, t) = f\left(q_{\parallel}^2 t^{\frac{1}{2}(1+\eta)}, q_{\perp}^2 t\right) . \quad (101)$$

While the system is normally diffusive with respect to the transverse directions, in the critical longitudinal direction typical length squares scale for long times as

$$\langle r_{\parallel}^2 \rangle \sim t^{\frac{1}{2}(1+\eta)} , \quad (102)$$

i.e. in comparison to the naively critical  $t^{\frac{1}{2}}$  (corresponding to the naive dynamical critical exponent  $z = 4$  from model B [23]) the spread of fluctuations in the driving force direction is enhanced, due to the positive  $\eta = \frac{2}{11}\epsilon + \mathcal{O}(\epsilon^2)$ . A comparison with the corresponding model for the longitudinal phase transition in a system without quenched disorder [5] shows the surprising result that the longitudinal phase transition is here continuous, evidenced by the existence of an infrared stable fixed point, whereas in the model without quenched disorder there is no infrared stable fixed point.

## 5 Summary and Outlook

We have analyzed the transverse and longitudinal phase transition in uniformly driven diffusive systems with quenched disorder. These systems show a wide variety of possible scenarios, because the symmetry properties of the random potential are an additional distinguishing feature to which universality class a model belongs. In the region of the transverse phase transition the three different random potentials I–III (Fig. 2) actually define three different models and in the noncritical region they still define two different models all of which are part of different universality classes.

Together with earlier investigations the renormalization group studies of an entire model class are hereby completed. This model class includes the driven diffusive systems with and without quenched disorder both in the critical regions of the transverse and longitudinal phase transition and in the noncritical region. Fig. 3 gives a graphical overview of the model class, where the single models are ordered chronologically from left to the right. The models in an ordered substrate [4–6], i.e. without quenched disorder, had been studied prior to this work for all three regions of the phase diagram mentioned above. The models for a system with quenched disorder in the noncritical region [7] had also been investigated. The other models of Fig. 3 have been studied in the present paper.

The upper critical dimension  $d_c$  is different from model to model and varies from 2 to 9. Below  $d_c$ , the vertex functions being typical statistical quantities of such systems show universal anomalous scaling behaviour on large length and time scales. The deviation from pure diffusive behaviour is characterized by the anomaly–exponent  $\eta$ . It indicates how strongly longitudinal lengths scale anomalously. In Fig. 3 the result for  $\eta$  in the highest calculated loop order is given for every model. Note that, due to Galilean invariance,  $\eta$  is even exact in all models without quenched disorder.

We emphasize the following results:

In all models of this model class (except for the longitudinal phase transition in a system without quenched disorder) the anomaly–exponent  $\eta$  is positive implying superdiffusive spreading of density fluctuations in the driving force direction.

A model with quenched disorder always has a higher upper critical dimension than the corresponding model without quenched disorder. Due to the field theoretic results, in the dimension interval between these two upper critical dimensions the quenched disorder is the reason for superdiffusive spread of

density fluctuations in the high temperature region and at the transverse phase transition, respectively. Notice that the anomalous diffusion of fluctuations is not directly connected with the behaviour of transport coefficients relating the mean current to the mean density, because a fluctuation–dissipation theorem (Einstein relation) does not hold in this strong nonequilibrium situation with quenched disorder. Within this model class we have not found a qualitative argument why disorder generates superdiffusion. We mention, however, a study of a one dimensional driven lattice gas [24, 25] where quenched disorder is not, as here, spatially fixed, but associated with moving particles. The authors found a superdiffusive spread of a jam behind the slowest particle and a superdiffusive spread of free spacing in front of it. Whether this situation can be transferred to our models by identifying the deepest potential valley and the highest potential mountain, respectively, with the slowest particle, should be a topic of further investigations, especially Monte Carlo simulations.

For the longitudinal phase transition there is no uniform statement. In the model without quenched disorder [5] no infrared stable fixed point has been found and some analytic arguments point to a discontinuous phase transition, whereas an according two dimensional lattice gas demonstrates a continuous phase transition in Monte Carlo simulations [26]. In the model with quenched disorder studied here, however, we find an infrared stable fixed point and thus a continuous longitudinal phase transition.

Despite the partially high upper critical dimensions it appears that the anomaly–exponent (when existing) may be extrapolated quite accurately into low dimensions. Two observations lend support to this procedure: first, the two–loop correction to  $\eta$  in the critical transverse model from Section 3.1 is small and second, the coefficients of  $\eta$  are small in all models.

For the two–loop calculation in critical models with quenched disorder a new technique has been developed enabling us to manipulate mixed  $\mathbf{q}^4$ –propagators and –correlators. This technique is based on an inverse Mellin transformation and is described for one model at the transverse phase transition in the Appendix. This method is applicable to all critical models with quenched disorder of this model class, but has only been performed for two models (Sec. 3.1 and 3.3). Furthermore we expect it to be useful for two–loop calculations in other physical problems where  $\mathbf{q}^4$ –propagators are involved. Monte Carlo simulations of two–dimensional driven diffusive lattice gases without quenched disorder [1, 2, 11, 12] are in excellent agreement with field theoretic predictions for the transverse phase transition and the noncritical

region [4–6]. For the transverse phase transition in systems with quenched disorder, however, there is a simulation study [27] that is, for two reasons, hardly compatible with the models investigated here by field theory. First, the quenched disorder was there modelled by randomly blocked sites and not by random potential barriers between the sites. Second, the concentration of blocked sites is so small that only the crossover behaviour between a system with and without quenched disorder was observed. Further, we mention a recent simulation for a noncritical system with quenched disorder [28].

It is desirable to compare the field theoretic results obtained here for the various critical models with corresponding Monte Carlo simulations that are still to be done. These simulations are a nontrivial challenge, because besides the average over a huge number of realizations of the quenched disorder it is to pay attention to the fact that the periodic boundary conditions usually used let pass a particle repeatedly through the system and let it see the same quenched disorder as before. By this unwanted correlations of the randomness enter into the simulational results that make it difficult to compare them with the field theoretic results that are based on the assumption of uncorrelated disorder. Therefore Monte Carlo simulations of driven diffusive systems with open boundaries already done for systems without quenched disorder [29] seem to be more appropriate.

We finally remark that we have extended the model class investigated here in the way that we allow for random particle sources and drains in the diffusive systems. The noncritical model without quenched disorder with such a particle nonconserving randomness had already been studied [13, 30]. Moreover we have analyzed the influence of nonconserving noise onto the critical behaviour in systems with and without quenched disorder which is demonstrated in a paper soon to be published [14].

## A Two-Loop Calculation of $\Gamma_{1,1}$

In the Appendix we explicitly show the two-loop calculation for the model that describes the transverse phase transition in an unsymmetric random potential (cf. Section 3.1). The graphical elements of the diagrammatic perturbation expansion are shown in Fig. 4 directly for the quasi-static model which is here used to facilitate the calculation. The  $\tilde{\varphi}$ -legs are indicated by an arrow and the  $q_{\parallel}$  of the vertex by a dash perpendicular to the propagator line. The mathematical expressions for the graphical elements are given by Equation (29).

In this model we have to calculate the primitively divergent vertex functions  $\Gamma_{1,1}$  and  $\Gamma_{1,2}$ . There are eight two-loop diagrams contributing to  $\Gamma_{1,1}$  (Fig. 5) and 25 two-loop diagrams contributing to  $\Gamma_{1,2}$  each of which obeys causality that forbids closed propagator loops. Momentum conservation demands that at each vertex the sum over all wave vectors is zero. Evaluation of these diagrams requires integration over all internal wave vectors.

While the one-loop calculation is easy to perform by standard methods, the two-loop calculation involving mixed  $\mathbf{q}^4$ -propagators requires more sophisticated tools and has not been described in literature. We introduce a technique that is based on an inverse Mellin transformation.

For  $\Gamma_{1,1}$  we have to compute the diagrams  $B_1^{(1,1)}$  to  $B_8^{(1,1)}$  from Fig. 5. We denote the external momentum by  $\mathbf{q}$  and the internal ones to be integrated over by  $\mathbf{p}$  and  $\mathbf{k}$ . As  $\Gamma_{1,1}$  is quadratically divergent because of CP-symmetry and dimensional reasons and the external  $\tilde{\varphi}$  already provides a factor  $q_{\parallel}$ , the parts of the integrands being proportional to  $q_{\parallel}$  contain all singularities. Therefore, the integrands are first expanded with respect to the external momentum  $q_{\parallel}$  to first order. For simplicity, we now substitute  $\rho^{\frac{1}{2}}p_{\parallel} \rightarrow p_{\parallel}$ ,  $\rho^{\frac{1}{2}}k_{\parallel} \rightarrow k_{\parallel}$  and from now on we omit the superscript “ $\circ$ ” to characterize unrenormalized quantities.

In the next step all even powers of  $p_{\parallel}$  and  $k_{\parallel}$  in the numerator of the integrands are written as  $p_{\parallel}^2 = [\mathbf{p}_{\perp}^2 (\mathbf{p}_{\perp}^2 + \tau_{\perp}) + p_{\parallel}^2] - \mathbf{p}_{\perp}^2 (\mathbf{p}_{\perp}^2 + \tau_{\perp})$  ( $k_{\parallel}^2$  analogously). The first term of the right hand side cancels against factors in the denominator. For all odd powers the half of the integrand is reflected with respect to  $k_{\parallel}$ . This step reduces the superficial degree of divergence of the  $\mathbf{p}$ - and  $\mathbf{k}$ -integration by 2. It is allowed because the integration runs over the whole  $k_{\parallel}$ -axis.



Then all integrals are reduced to the two types of integrals

$$\begin{aligned}
I(\alpha, \beta, \gamma, \delta, \mu, \nu) &:= \tag{103} \\
&\int_{\mathbf{p}} \frac{\mathbf{p}_{\perp}^{2\alpha}}{[\mathbf{p}_{\perp}^2(\mathbf{p}_{\perp}^2 + \tau_{\perp}) + p_{\parallel}^2]^{\beta}} \int_{\mathbf{k}} \frac{(\mathbf{p}_{\perp} - \mathbf{k}_{\perp})^{2\gamma}}{[(\mathbf{p}_{\perp} - \mathbf{k}_{\perp})^4 + (p_{\parallel} - k_{\parallel})^2]^{\delta}} \frac{\mathbf{k}_{\perp}^{2\mu}}{[\mathbf{k}_{\perp}^4 + k_{\parallel}^2]^{\nu}} \\
F(A; \alpha, \beta, \gamma, \delta, \mu, \nu) &:= \int_{\mathbf{p}} \frac{p_{\parallel}^A \mathbf{p}_{\perp}^{2\alpha}}{[\mathbf{p}_{\perp}^2(\mathbf{p}_{\perp}^2 + \tau_{\perp}) + p_{\parallel}^2]^{\beta}} \\
&\cdot \int_{\mathbf{k}} \frac{k_{\parallel} \mathbf{k}_{\perp}^{2\mu}}{[\mathbf{k}_{\perp}^4 + k_{\parallel}^2]^{\nu}} \left[ \frac{(\mathbf{p}_{\perp} - \mathbf{k}_{\perp})^{2\gamma}}{[(\mathbf{p}_{\perp} - \mathbf{k}_{\perp})^4 + (p_{\parallel} - k_{\parallel})^2]^{\delta}} - \frac{(\mathbf{p}_{\perp} - \mathbf{k}_{\perp})^{2\gamma}}{[(\mathbf{p}_{\perp} - \mathbf{k}_{\perp})^4 + (p_{\parallel} + k_{\parallel})^2]^{\delta}} \right]
\end{aligned}$$

the arguments of which can be 0, 1, 2,...

As the integrands are already expanded with respect to  $q_{\parallel}$ , the whole integration over  $\mathbf{p}$  and  $\mathbf{k}$  is at most logarithmically divergent. The integration variables are chosen such that the  $\mathbf{p}$ -subintegration is always primitively convergent, i.e., the naive dimension  $\delta_{\mathbf{p}}$  of this integration (measured in powers of the external momentum scale  $\mu$ ) is negative. In the integrals of both types the  $\mathbf{k}$ -integration is at most logarithmically divergent.

Due to these naive dimensions of the  $\mathbf{p}$ -,  $\mathbf{k}$ - and the whole integration it is possible (and necessary for the following calculus) to set  $\tau_{\perp} = 0$  in the  $\mathbf{k}$ -integration, because the  $\tau_{\perp} \neq 0$ -parts only provide convergent contributions. The sum of the two-loop diagrams for  $\Gamma_{1,1}$  expressed by the integral types  $I$  and  $F$  reads

$$\begin{aligned}
\sum_{i=1}^8 B_i^{(1,1)} &= 4 \frac{g^4}{\rho^2} q_{\parallel}^2 [3I(1, 3, 0, 1, 1, 2) - 3I(1, 3, 0, 1, 3, 3) - 2I(3, 4, 0, 1, 1, 2) \\
&+ 2I(3, 4, 0, 1, 3, 3) - 2\tau_{\perp} I(2, 4, 0, 1, 1, 2) + 2\tau_{\perp} I(2, 4, 0, 1, 3, 3) \\
&+ \frac{1}{2} I(0, 2, 1, 2, 1, 2) - \frac{3}{2} I(2, 3, 1, 2, 1, 2) + I(4, 4, 1, 2, 1, 2) \\
&- F(3; 1, 4, 0, 1, 1, 3) - \frac{1}{2} F(1; 1, 3, 0, 1, 1, 3) + F(1; 1, 4, 1, 2, 0, 1)]. \tag{104}
\end{aligned}$$

By factorizing the  $\mathbf{q}^4$ -denominators in  $I$  and  $F$  into transverse and longitudinal parts we are in the position to apply the successful methods that are used for  $\mathbf{q}^2$ -propagators and -correlators. This factorization is done by the Mellin transformation. We demonstrate the method for the integral type  $I$

in detail. The calculation of  $F$  goes analogously.

The Mellin transformation of the function  $(a+x)^{-\alpha}$  is

$$\int_0^\infty dx x^{t-1} (a+x)^{-\alpha} = \frac{\Gamma(t)\Gamma(\alpha-t)}{\Gamma(\alpha)} a^{t-\alpha}, \quad (105)$$

where the conditions  $a > 0$  and  $0 < \text{Re}(t) < \text{Re}(\alpha)$  must be fulfilled [31]. The corresponding inverse Mellin transformation

$$(a+x)^{-\alpha} = \int_{t_0-i\infty}^{t_0+i\infty} \frac{dt}{2\pi i} \left( \frac{\Gamma(t)\Gamma(\alpha-t)}{\Gamma(\alpha)} a^{t-\alpha} \right) x^{-t}, \quad (106)$$

where the integration path parallel to the imaginary axis is restricted by  $0 < t_0 < \text{Re}(\alpha)$  [31], proves to be the appropriate tool to factorize the denominators in  $I$ .

First we only treat the  $\mathbf{k}$ -integration of the integral type  $I$  (103) and apply the inverse Mellin transformation to both denominators

$$\begin{aligned} I_{\mathbf{k}} &:= \int_{\mathbf{k}} \frac{(\mathbf{p}_\perp - \mathbf{k}_\perp)^{2\gamma}}{[(\mathbf{p}_\perp - \mathbf{k}_\perp)^4 + (p_\parallel - k_\parallel)^2]^\delta} \frac{\mathbf{k}_\perp^{2\mu}}{[\mathbf{k}_\perp^4 + k_\parallel^2]^\nu} \\ &= \int_{t_0-i\infty}^{t_0+i\infty} \frac{dt}{2\pi i} \int_{s_0-i\infty}^{s_0+i\infty} \frac{ds}{2\pi i} \frac{\Gamma(t)\Gamma(\delta-t)\Gamma(s)\Gamma(\nu-s)}{\Gamma(\delta)\Gamma(\nu)} \\ &\quad \cdot \int_{\mathbf{k}} \frac{1}{[k_\parallel^2]^s [(p_\parallel - k_\parallel)^2]^t} \frac{1}{[\mathbf{k}_\perp^2]^{2(\nu-s)-\mu} [(\mathbf{p}_\perp - \mathbf{k}_\perp)^2]^{2(\delta-t)-\gamma}}. \end{aligned} \quad (107)$$

In the integrand transverse and longitudinal momenta are now separated and only quadratic. The  $\mathbf{k}$ -integration can now be performed with the help of the usual Feynman relations

$$\begin{aligned} \frac{1}{A^\alpha} &= \frac{1}{\Gamma(\alpha)} \int_0^\infty ds s^{\alpha-1} e^{-sA} \\ \frac{1}{\prod_i A_i^{\alpha_i}} &= \frac{\Gamma(\sum_i \alpha_i)}{\prod_i \Gamma(\alpha_i)} \int_0^1 \prod_i dx_i x_i^{\alpha_i-1} \frac{\delta(\sum_i x_i - 1)}{[\sum_i x_i A_i]^{\sum_i \alpha_i}}, \end{aligned} \quad (108)$$

where  $\Gamma(\alpha)$  is Euler's  $\Gamma$  function. The result reads

$$\begin{aligned} I_{\mathbf{k}} &= \frac{1}{2} \frac{\mathcal{O}_{d-1}}{(2\pi)^d} \Gamma\left(\frac{1}{2}\right) \Gamma\left(\frac{d-1}{2}\right) \int_{t_0-i\infty}^{t_0+i\infty} \frac{dt}{2\pi i} \int_{s_0-i\infty}^{s_0+i\infty} \frac{ds}{2\pi i} \frac{\Gamma(t)\Gamma(\delta-t)\Gamma(s)\Gamma(\nu-s)}{\Gamma(\delta)\Gamma(\nu)} \\ &\quad \cdot \frac{\Gamma(s+t-\frac{1}{2})\Gamma(\frac{1}{2}-s)\Gamma(\frac{1}{2}-t)}{\Gamma(s)\Gamma(t)\Gamma(1-s-t)} \frac{\Gamma(2\nu+2\delta-\mu-\gamma-\frac{d-1}{2}-2(s+t))}{\Gamma(2(\nu-s)-\mu)\Gamma(2(\delta-t)-\gamma)} \end{aligned}$$

$$\begin{aligned}
& \cdot \frac{\Gamma(\frac{d-1}{2} - 2(\nu - s) + \mu) \Gamma(\frac{d-1}{2} - 2(\delta - t) + \gamma)}{\Gamma(d - 1 - 2\nu - 2\delta + \mu + \gamma + 2(s + t))} \\
& \cdot |p_{\parallel}|^{1-2(s+t)} |\mathbf{p}_{\perp}|^{d-1+4(s+t-\nu-\delta)+2(\gamma+\mu)} .
\end{aligned} \tag{109}$$

The  $\mathbf{k}$ -integral exists under the conditions

$$\begin{aligned}
2(s_0 + t_0) &> 1 \\
s_0 < \frac{1}{2} & \quad t_0 < \frac{1}{2} \\
4(\nu + \delta - (s_0 + t_0)) - 2(\mu + \gamma) &> d - 1 \\
d - 1 - 4(\nu - s_0) + 2\mu &> 0 \\
d - 1 - 4(\delta - t_0) + 2\gamma &> 0
\end{aligned} \tag{110}$$

which prevent UV and IR divergences, respectively, at the  $k_{\parallel}$ - and  $\mathbf{k}_{\perp}$ -integration. These conditions restrict the complex integration paths of the  $s$ - and  $t$ -integration which are here dependent on the spatial dimension, due to the dimensional regularization.

The result of the  $\mathbf{k}$ -integration is according to Equation (109) proportional to powers of  $|p_{\parallel}|$  and  $|\mathbf{p}_{\perp}|$  with exponents that are dependent on  $s$ ,  $t$ , and  $d$ . Thus, the remaining  $\mathbf{p}$ -integration is analogous to the one-loop problem, up to changed exponents. It is straightforwardly performed and we obtain for  $I$

$$\begin{aligned}
I(\alpha, \beta, \gamma, \delta, \mu, \nu) &= C_d \frac{\Gamma(2(\beta + \delta + \nu) - (\alpha + \gamma + \mu) - (d + 1))}{\tau_{\perp}^{2(\beta + \delta + \nu) - (\alpha + \gamma + \mu) - (d + 1)}} \\
& \cdot \int_{t_0 - i\infty}^{t_0 + i\infty} \frac{dt}{2\pi i} \int_{s_0 - i\infty}^{s_0 + i\infty} \frac{ds}{2\pi i} \Gamma(2\nu + 2\delta - \mu - \gamma - \frac{d-1}{2} - 2(s+t)) \Gamma(s+t - \frac{1}{2}) \\
& \cdot \Gamma(\delta - t) \Gamma(\nu - s) \Gamma(\frac{1}{2} - s) \Gamma(\frac{1}{2} - t) \frac{\Gamma(d + s + t + \alpha + \gamma + \mu - \beta - 2\delta - 2\nu)}{\Gamma(d - 1 - 2\nu - 2\delta + \mu + \gamma + 2(s+t))} \\
& \cdot \frac{\Gamma(\frac{d-1}{2} - 2(\nu - s) + \mu) \Gamma(\frac{d-1}{2} - 2(\delta - t) + \gamma)}{\Gamma(2(\nu - s) - \mu) \Gamma(2(\delta - t) - \gamma)} , \tag{111}
\end{aligned}$$

where  $C_d = \frac{1}{4} \left( \frac{\mathcal{O}_{d-1}}{(2\pi)^d} \right)^2 \frac{\Gamma(\frac{1}{2}) \Gamma(\frac{d-1}{2})}{\Gamma(\beta) \Gamma(\delta) \Gamma(\nu)}$  is a constant that is different for every  $I$  and depends on the dimension. The conditions for the existence of the  $\mathbf{p}$ -integration are

$$\begin{aligned}
1 - (s_0 + t_0) &> 0 \\
d + s_0 + t_0 + \alpha + \gamma + \mu - \beta - 2\delta - 2\nu &> 0 \\
2(\beta + \delta + \nu) - (\alpha + \gamma + \mu) - (d + 1) &> 0 .
\end{aligned} \tag{112}$$

After the momentum integrations there remain parameter integrations with respect to the Mellin variables  $s$  and  $t$  over parallels to the imaginary axis. The complex integration paths and the spatial dimension  $d$  are restricted by the conditions (110) and (112). With  $\epsilon = 9 - d$  we obtain from the first four inequalities of (110)

$$\frac{1}{2} < s_0 + t_0 < \delta + \nu - \frac{1}{2}(\gamma + \mu) - 2 + \frac{\epsilon}{4}, \quad (113)$$

where  $s_0 < \frac{1}{2}$ ,  $t_0 < \frac{1}{2}$ . All other conditions are satisfied for all  $I$  of Equation (104), if  $0 < \epsilon < 2$ .

Since the sum  $s_0 + t_0$  appears in the inequality (113) we transform to the new integration variables

$$z := s + t \quad w := \frac{1}{2}(s - t). \quad (114)$$

The integration paths are now determined by

$$\begin{aligned} \frac{1}{2} < z_0 < \delta + \nu - \frac{1}{2}(\gamma + \mu) - 2 + \frac{\epsilon}{4} \\ |w_0| < \frac{1}{4}. \end{aligned} \quad (115)$$

After this substitution Equation (111) gives

$$\begin{aligned} I(\alpha, \beta, \gamma, \delta, \mu, \nu) &= C_d \frac{\Gamma(2(\beta + \delta + \nu) - (\alpha + \gamma + \mu) - (d + 1))}{\tau_{\perp}^{2(\beta + \delta + \nu) - (\alpha + \gamma + \mu) - (d + 1)}} \\ &\cdot \int_{z_0 - i\infty}^{z_0 + i\infty} \frac{dz}{2\pi i} \int_{w_0 - i\infty}^{w_0 + i\infty} \frac{dw}{2\pi i} \Gamma(2\nu + 2\delta - \mu - \gamma - \frac{d-1}{2} - 2z) \Gamma(z - \frac{1}{2}) f(z, w; \epsilon), \end{aligned} \quad (116)$$

where the abbreviation

$$\begin{aligned} f(z, w; \epsilon) &:= \Gamma(\delta - \frac{z}{2} + w) \Gamma(\nu - \frac{z}{2} - w) \Gamma(\frac{1}{2} - \frac{z}{2} - w) \Gamma(\frac{1}{2} - \frac{z}{2} + w) \\ &\cdot \frac{\Gamma(\frac{8-\epsilon}{2} - 2(\nu - \frac{z}{2} - w) + \mu) \Gamma(\frac{8-\epsilon}{2} - 2(\delta - \frac{z}{2} + w) + \gamma)}{\Gamma(2(\nu - \frac{z}{2} - w) - \mu) \Gamma(2(\delta - \frac{z}{2} + w) - \gamma)} \\ &\cdot \frac{\Gamma(9 - \epsilon + z + \alpha + \gamma + \mu - \beta - 2\delta - 2\nu)}{\Gamma(8 - \epsilon - 2\nu - 2\delta + \mu + \gamma + 2z)} \end{aligned} \quad (117)$$

denotes the part of the integrand that is free of poles.

To extract the divergent parts of  $I$  we have to distinguish two cases.

Case 1: The  $\mathbf{k}$ -integration is primitively convergent.

In this case the parameters satisfy

$$\nu + \delta - \frac{1}{2}(\gamma + \mu) = 3 , \quad (118)$$

which is true for  $I(0, 2, 1, 2, 1, 2)$ ,  $I(2, 3, 1, 2, 1, 2)$ , and  $I(4, 4, 1, 2, 1, 2)$  from Equation (104). According to Equation (115) this means for the constant  $z_0$  which determines the integration path

$$\frac{1}{2} < z_0 < 1 + \frac{\epsilon}{4} . \quad (119)$$

For these  $I$  the whole integration over  $\mathbf{p}$  and  $\mathbf{k}$  is logarithmically divergent so that their parameters fulfill the equation

$$2(\beta + \delta + \nu) - (\alpha + \gamma + \mu) - (d + 1) = \epsilon . \quad (120)$$

Thus, the coefficient  $\Gamma(\epsilon) = \frac{1}{\epsilon}\Gamma(1 + \epsilon)$  of the double integral over  $z$  and  $w$  (116) contains an  $\epsilon$ -pole, whereas the double integral itself is convergent, as the integrand is free of poles even in the limit  $\epsilon \rightarrow 0$  and the real part of the integration path can be chosen between  $\frac{1}{2}$  and 1 according to Equation (119). The double integral in Equation (116) can therefore be computed at  $\epsilon = 0$ , because together with the  $\epsilon$ -pole as coefficient only convergent contributions are produced for  $\epsilon \neq 0$ . The convergence of the double integral is ensured by the asymptotic behaviour of the  $\Gamma$  function with complex arguments [32]

$$\lim_{|y| \rightarrow \infty} |\Gamma(x + iy)| e^{\frac{\pi}{2}|y|} |y|^{\frac{1}{2}-x} = (2\pi)^{\frac{1}{2}} . \quad (121)$$

Due to the accumulation of  $\Gamma$  functions we are not able to perform the integrations with respect to  $z$  and  $w$  analytically. Hence, each of the three  $I$  is computed numerically for  $\epsilon = 0$ .

Case 2: The  $\mathbf{k}$ -integration is logarithmically divergent.

In this case the parameters are restricted to

$$\nu + \delta - \frac{1}{2}(\gamma + \mu) = \frac{5}{2} , \quad (122)$$

which is correct for the remaining  $I$  from Equation (104). According to Equation (115) the integration path is here restricted by

$$\frac{1}{2} < z_0 < \frac{1}{2} + \frac{\epsilon}{4} . \quad (123)$$

In the limit  $\epsilon \rightarrow 0$  the integration path is trapped by this condition between the poles of the integrand (116) at  $z = \frac{1}{2}$  and  $z = \frac{1}{2} + \frac{\epsilon}{4}$ . In order to extract the  $\epsilon$ -poles the complex integration path is decomposed into two parts (as shown graphically in Fig. 6): The first part is a line parallel to the imaginary axis with an arc to the left of the singularity  $z = \frac{1}{2}$ , while the second part is a circle around  $z = \frac{1}{2}$ . The  $z$ -integral over the circle gives the residuum at  $z = \frac{1}{2}$ .

This way we obtain from Equation (116)

$$I(\alpha, \beta, \gamma, \delta, \mu, \nu) = C_d \frac{\Gamma(2(\beta + \delta + \nu) - (\alpha + \gamma + \mu) - (d + 1))}{\tau_{\perp}^{2(\beta + \delta + \nu) - (\alpha + \gamma + \mu) - (d + 1)}} \quad (124)$$

$$\cdot \left[ \int_{z'_0 - i\infty}^{z'_0 + i\infty} \frac{dz}{2\pi i} \int_{w_0 - i\infty}^{w_0 + i\infty} \frac{dw}{2\pi i} \Gamma(1 + \frac{\epsilon}{2} - 2z) \Gamma(z - \frac{1}{2}) f(z, w; \epsilon) \right.$$

$$\left. + \Gamma(\frac{\epsilon}{2}) \int_{w_0 - i\infty}^{w_0 + i\infty} \frac{dw}{2\pi i} f(z = \frac{1}{2}, w; \epsilon) \right],$$

Naturally, the integration path of the  $z$ -integration is again chosen as a parallel to the imaginary axis, whose real part  $z'_0$  now lies between  $-\frac{1}{2}$  and  $\frac{1}{2}$ . After the integration path is changed, both the double integral over  $z$  and  $w$  and the single integral over  $w$  are eventually convergent. Only the coefficients of the integrals contain the  $\epsilon$ -poles. For the further calculation we have again to distinguish two cases.

a) The whole integration is logarithmically divergent.

This is the case for the integrals  $I(1, 3, 0, 1, 1, 2)$ ,  $I(1, 3, 0, 1, 3, 3)$ ,  $I(3, 4, 0, 1, 1, 2)$ , and  $I(3, 4, 0, 1, 3, 3)$  from Equation(104). Their parameters satisfy Equation (120) so that in front of the entire bracket there is an  $\epsilon$ -pole due to  $\Gamma(\epsilon)$ .

For every single  $I$  the double integral is finally calculated for  $\epsilon = 0$  numerically and provides the coefficients of simple  $\epsilon$ -poles. Parts of the integrand with  $\epsilon \neq 0$  lead to convergent contributions and are therefore omitted.

The coefficient  $\Gamma(\epsilon)\Gamma(\frac{\epsilon}{2})$  of the simple integral, however, contains an  $\epsilon^2$ -pole. Hence, the integrand  $f(z = \frac{1}{2}, w; \epsilon)$  must be expanded with respect to  $\epsilon$  up to the first order

$$f(z = \frac{1}{2}, w; \epsilon) = \frac{\Gamma(\frac{19}{2} - \epsilon + \alpha + \gamma + \mu - \beta - 2\delta - 2\nu)}{\Gamma(9 - \epsilon - 2\nu - 2\delta + \mu + \gamma)} \Gamma(\delta - \frac{1}{4} + w)$$

$$\cdot \Gamma(\nu - \frac{1}{4} - w) \Gamma(\frac{1}{4} - w) \Gamma(\frac{1}{4} + w) \frac{\Gamma(\frac{9-\epsilon}{2} - 2(\nu - w) + \mu) \Gamma(\frac{9-\epsilon}{2} - 2(\delta + w) + \gamma)}{\Gamma(2(\nu - \frac{1}{4} - w) - \mu) \Gamma(2(\delta - \frac{1}{4} + w) - \gamma)}$$

$$\begin{aligned}
&= \frac{\Gamma(\beta - \frac{1}{2} - \epsilon)}{\Gamma(4 - \epsilon)} \Gamma(\delta - \frac{z}{2} + w) \Gamma(\nu - \frac{z}{2} - w) \Gamma(\frac{1}{2} - \frac{z}{2} - w) \Gamma(\frac{1}{2} - \frac{z}{2} + w) \\
&\quad \cdot \left[ 1 - \frac{\epsilon}{2} (\Psi(2\delta - \frac{1}{2} + 2w - \gamma) + \Psi(2\nu - \frac{1}{2} - 2w - \mu)) + \mathcal{O}(\epsilon^2) \right] , \quad (125)
\end{aligned}$$

where  $\Psi(x) = \frac{\Gamma'(x)}{\Gamma(x)}$  denotes Euler's  $\Psi$  function and the relations (120) and (122) have been used. The integral of the zeroth order in  $\epsilon$  provides the coefficients of the  $\epsilon^2$ -poles and can even be executed analytically [32]

$$\begin{aligned}
\int_{w_0-i\infty}^{w_0+i\infty} \frac{dw}{2\pi i} \Gamma(\delta - \frac{1}{4} + w) \Gamma(\nu - \frac{1}{4} - w) \Gamma(\frac{1}{4} - w) \Gamma(\frac{1}{4} + w) &= \quad (126) \\
&\quad \frac{\Gamma(\delta) \Gamma(\delta + \nu - \frac{1}{2}) \Gamma(\nu) \Gamma(\frac{1}{2})}{\Gamma(\delta + \nu)} .
\end{aligned}$$

The integral of the first order in  $\epsilon$  yields the coefficients of the  $\epsilon$ -poles and is numerically calculated for every single  $I$  that belongs to this case 2 a).

b) The whole integration is primitively convergent.

This statement is true for  $\tau_{\perp} I(2, 4, 0, 1, 1, 2)$  and  $\tau_{\perp} I(2, 4, 0, 1, 3, 3)$  in Equation (104). Here the parameters have the property

$$2(\beta + \delta + \nu) - (\alpha + \gamma + \mu) - (d + 1) = 1 + \epsilon , \quad (127)$$

i.e. in front of the brackets in Equation (124) the coefficient is  $\Gamma(1 + \epsilon)$  and consequently there is no  $\epsilon$ -pole.

Therefore the double integral needs not to be computed, as it only leads to convergent contributions. The simple integral can be evaluated at  $\epsilon = 0$  because the coefficient contains only a simple  $\epsilon$ -pole. Due to the relation (122) that is also valid here, the simple integral is reduced to the one already solved in Equation (126) analytically.

Now all integrals of type  $I$  from Equation (104) have been calculated. The way to solve the integrals of type  $F$  is step by step analogous to the method presented for type  $I$ .  $F(3; 1, 4, 0, 1, 1, 3)$  and  $F(1; 1, 3, 0, 1, 1, 3)$  from Equation (104) belong to case 1, whereas  $F(1; 1, 4, 1, 2, 0, 1)$  belongs to case 2 a).

Finally we present the sum of the two-loop diagrams for  $\Gamma_{1,1}$  up to convergent parts (cf. (30))

$$\sum_{i=1}^8 B_i^{(1,1)} = 4 \frac{g^4}{\rho^2} q_{\parallel}^2 A_{\epsilon}^2 \frac{\tau_{\perp}^{-\epsilon}}{\epsilon^2} \left( \frac{1}{18} - 0.01199\epsilon \right) . \quad (128)$$

The 25 two-loop diagrams of the primitively divergent  $\Gamma_{1,2}$  again only lead to integrals of type  $I$  and  $F$

$$\begin{aligned}
\sum_{i=1}^{25} B_i^{(1,2)} = & -4i \frac{g^5}{\rho^3} q_{\parallel} [3I(1, 3, 0, 1, 1, 2) - I(1, 3, 1, 2, 2, 2) - 3I(3, 4, 0, 1, 1, 2) \\
& + I(3, 4, 1, 2, 2, 2) - 2I(1, 3, 0, 1, 3, 3) + 2I(3, 4, 0, 1, 3, 3) \\
& - 3\tau_{\perp} I(2, 4, 0, 1, 1, 2) + 2\tau_{\perp} I(2, 4, 0, 1, 3, 3) + \tau_{\perp} I(2, 4, 1, 2, 2, 2) \\
& - \frac{1}{2} I(0, 2, 1, 2, 1, 2) + I(2, 3, 1, 2, 1, 2) - \frac{1}{2} I(4, 4, 1, 2, 1, 2) \\
& - F(3; 1, 4, 0, 1, 1, 3) + F(3; 0, 3, 1, 2, 1, 3) + 2F(3; 1, 5, 1, 2, 0, 1)], \\
& (129)
\end{aligned}$$

which can be evaluated with the methods demonstrated for  $\Gamma_{1,1}$ . This concludes the two-loop calculation.



### Acknowledgement

The authors thank K. Oerding and B. Schmittmann for illuminating discussions. This work has been supported by the DFG under SFB 237 (Unordnung und Grosse Fluktuationen).

## References

- [1] S. Katz, J.L. Lebowitz, and H. Spohn. *Phys. Rev. B*, **28**:1655, 1983.
- [2] S. Katz, J.L. Lebowitz, and H. Spohn. *J. Stat. Phys.*, **34**:497, 1984.
- [3] B. Schmittmann and R.K.P. Zia. Statistical mechanics of driven diffusive systems. In C. Domb and J. Lebowitz, editors, *Phase Transitions and Critical Phenomena*, volume 17. Academic Press, London, 1994.
- [4] H.K. Janssen and B. Schmittmann. *Zeitschrift für Physik B –Condensed Matter*, **63**:517, 1986.
- [5] H.K. Janssen and B. Schmittmann. *Zeitschrift für Physik B –Condensed Matter*, **64**:503, 1986.
- [6] K.-T. Leung and J.L. Cardy. *J. Stat. Phys.*, **44**:567, 1087, 1986.
- [7] V. Becker and H.K. Janssen. *Europhys. Lett*, **19**:13, 1992.
- [8] B. Schmittmann and K.E. Bassler. *Phys. Rev. Lett.*, **77**:3581, 1996.
- [9] B. Schmittmann and C.A. Laberge. *Europhys. Lett.*, **37**:559, 1997.
- [10] J. Marro, J.L. Lebowitz, H. Spohn, and M.H. Kalos. *J. Stat. Phys.*, **38**:725, 1985.
- [11] K.-T. Leung. *Phys. Rev. Lett.*, **66**:453, 1991.
- [12] K.-T. Leung. *Int. J. Mod. Phys. C*, **3**:367, 1992.
- [13] V. Becker and H.K. Janssen. *Phys. Rev. E*, **50**:1114, 1994.
- [14] V. Becker and H.K. Janssen. Field theory of driven diffusive systems with random particle sources. *to be published*.
- [15] H.K. Janssen. *Zeitschrift für Physik B*, **23**:377, 1976.

- [16] C. De Dominicis. *J. Physique (Paris) C*, **1**:247, 1976.
- [17] H.K. Janssen. Field-theoretic method applied to critical dynamics. In C.P. Enz, editor, *Dynamical Critical Phenomena and Related Topics*, volume 104 of *Springer Lecture Notes in Physics*. Springer, 1979.
- [18] H.K. Janssen. On the renormalized field theory of nonlinear critical relaxation. In G. Györgyi, I. Kondor, L. Sasvári, and T. Tél, editors, *From Phase Transitions to Chaos*, Topics of Modern Statistical Physics. World Scientific, 1992.
- [19] R. Bausch, H.K. Janssen, and H. Wagner. *Zeitschrift für Physik B*, **24**:113, 1976.
- [20] C. De Dominicis and L. Peliti. *Phys. Rev. B*, **18**:353, 1978.
- [21] P.C. Martin, E.D. Siggia, and H.A. Rose. *Phys. Rev. A*, **8**:423, 1973.
- [22] D.J. Amit. *Field Theory, the Renormalization Group, and Critical Phenomena*. World Scientific, Singapore, 1984.
- [23] P.C. Hohenberg and B.I. Halperin. *Rev. Mod. Phys.*, **49**:435, 1977.
- [24] J. Krug and P.A. Ferrari. *J. Phys A: Math. Gen.*, **29**:L465, 1996.
- [25] M.R. Evans. *J. Phys. A: Math. Gen.*, **30**:5669, 1997.
- [26] K.E. Bassler and R.K.P. Zia. *J. Stat. Phys*, **80**:499, 1995.
- [27] K.B. Lauritsen and H.C. Fogedby. *Phys. Rev. E*, **47**:1563, 1993.
- [28] G. Tripathy and M. Barma. *Phys. Rev. E*, **58**:1911, 1998.
- [29] H.K. Janssen and K. Oerding. *Phys. Rev. E*, **58**:1446, 1998.
- [30] T. Hwa and M. Kardar. *Phys. Rev. A*, **45**:7002, 1992.
- [31] A. Erdelyi, W. Magnus, F. Oberhettinger, and F.G. Tricomi. *Tables of integral transforms*, volume 1. McGraw-Hill, New York, 1954.
- [32] I.S. Gradshteyn and I.M. Ryzhik. *Table of Integrals, Series, and products*. Academic Press, New York, 4. edition, 1980.

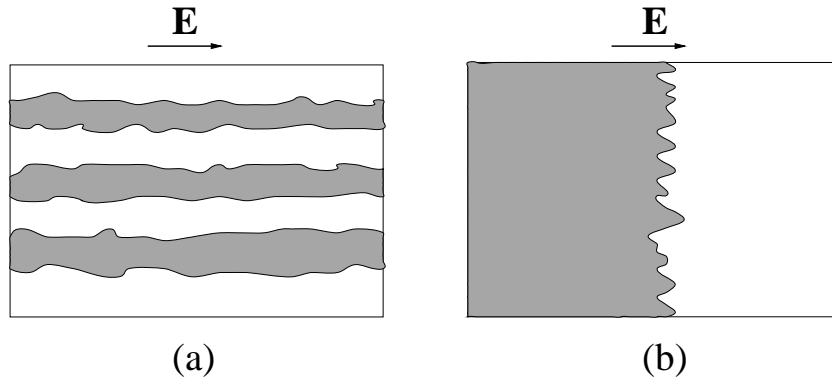


Figure 1: Typical configurations of transverse (a) and longitudinal (b) ordered phase. Regions of high density are shaded.

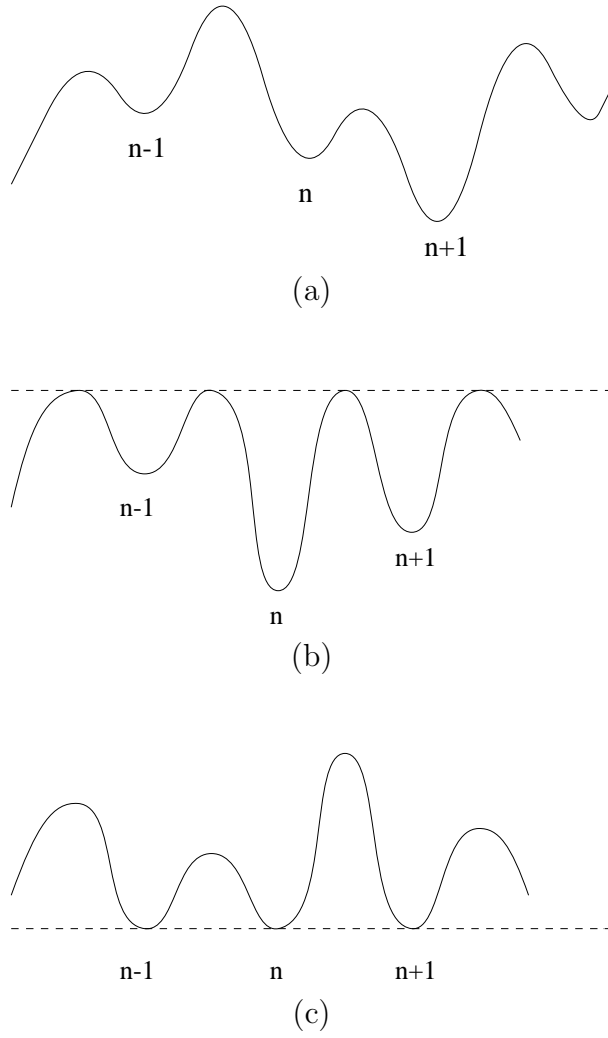
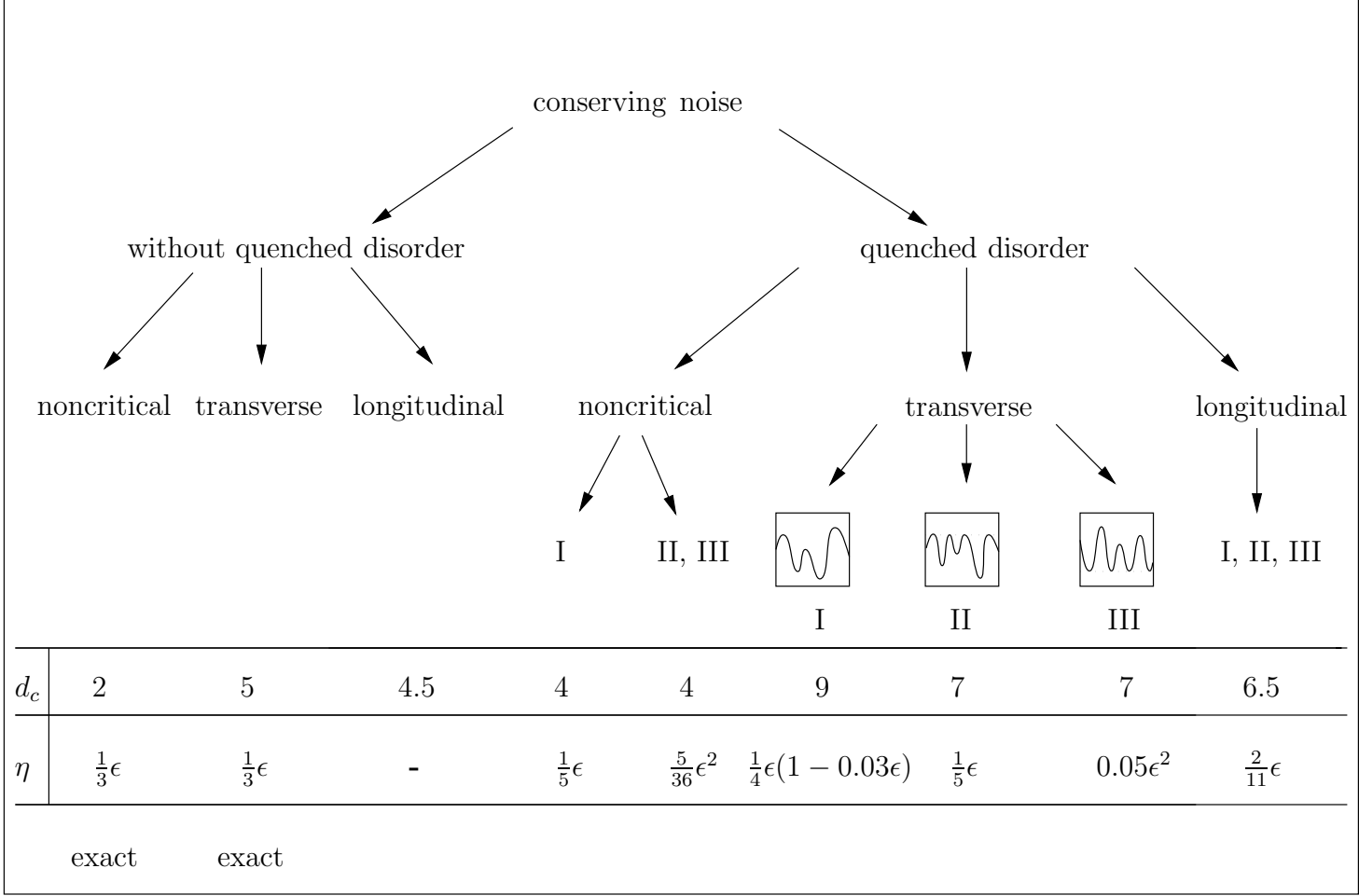


Figure 2: (a) Unsymmetric random potential, (b) random potential with equally high mountains, and (c) random potential with equally deep valleys.

Figure 3: Model class of driven diffusive systems with conserving noise.

45



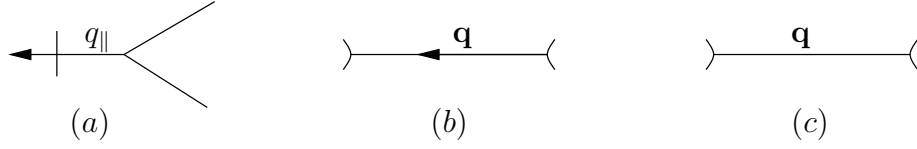


Figure 4: The graphical elements of perturbation theory in the quasi-static model: (a) vertex, (b) Gaussian propagator, and (c) Gaussian correlator.

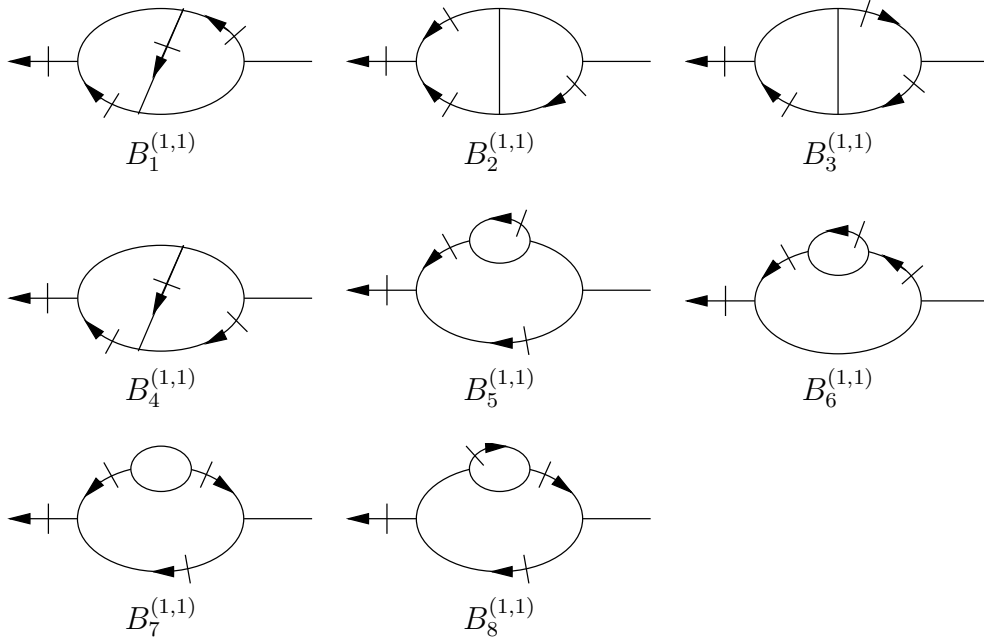


Figure 5: All two-loop diagrams of  $\Gamma_{1,1}$  obeying causality. The symmetry factor of  $B_7^{(1,1)}$  is  $\frac{1}{2}$ , whereas it is 1 for all other diagrams.

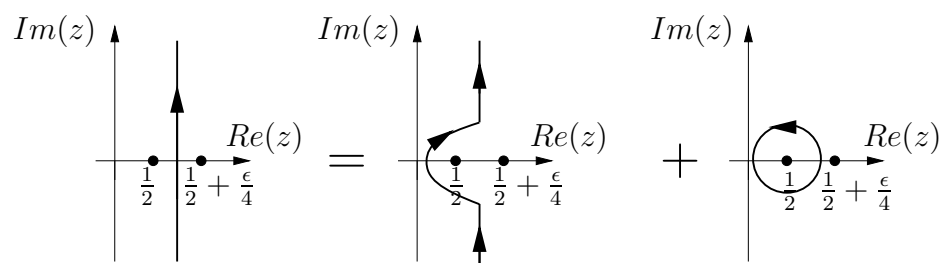


Figure 6: The complex integration path lying between two poles is decomposed into two parts.